

Genesis of the Olympias Carbonate-Hosted Pb-Zn(Au,Ag) Sulfide Ore Deposit, Eastern Chalkidiki Peninsula, Northern Greece

S. I. KALOGEROPOULOS, S. P. KILIAS, D. C. BITZIOS,

Institute of Geology and Mineral Exploration (IGME), 70 Mesoghion Street, Athens 115 27, Greece

M. NICOLAOU,

The Hellenic Chemical Products and Fertilizers Company, Ltd., 20 Amalias Avenue, Athens 105 57, Greece

AND R. A. BOTH

Department of Geology and Geophysics, University of Adelaide, G.P.O. Box 498, Adelaide, South Australia 5001, Australia

Abstract

The Olympias, Madem Lakos, and Mavres Petres Pb-Zn(Au,Ag) sulfide ore deposits are developed in calcitic-rhodochrositic marbles of the Paleozoic or older Kerdilia Formation, eastern Chalkidiki Peninsula, Northern Greece. Regionally the ore distribution is structurally controlled.

The geologic setting of the ores consists predominantly of marbles, biotite-hornblende gneisses, and amphibolites. These rocks have been regionally deformed and metamorphosed to amphibolite facies. This event in the Kerdilia Formation seems to have lasted until the early Tertiary and culminated in anatexis and calc-alkaline magmatism. These phenomena are represented by deformed and undeformed varieties of pegmatites-aplites, lamprophyre dikes, and the 30-Ma Stratoni granodiorite. This stage is also characterized by contact metamorphic phenomena and retrogression to the greenschist facies.

Geochemical and mineralogical evidence indicates that the biotite gneisses are of either sedimentary or igneous origin; the amphibolites have been derived from basaltic to basaltic-andesite protoliths with midocean ridge basalt geochemical affinity; the pegmatites-aplites are of anatectic origin from a magma produced at deeper crustal levels; the lamprophyre dikes are considered to be mantle derivatives; and the Stratoni granodiorite has been formed from a magma of hybrid nature consisting of mantle- and crustlike components.

The Olympias deposit is generally strata bound or fracture controlled and in places stratiform. It develops along the upper contact of the lower marble unit with the overlying biotite gneiss and within this marble; it strikes north-northeast for 1,500 m, dips 30° to 35° southeast to a depth of at least 300 m, and has an average thickness of 12 m. The contacts between the ore mineralization and the host marble are sharp, concordant or discordant to the foliation. However, in all cases a chemical reaction front in the marble is present.

The Olympias deposit occurs in undeformed and deformed varieties. The former predominates and is present in several forms such as cavity- and fracture-filling, banded, or disseminated. The latter is of limited presence and occurs as banded or in veins exhibiting shear folding and brecciation. S-type deformation in skarns near the 30-Ma Stratoni granodiorite and regional deformation-metamorphism data may place the time of ore formation in the Tertiary period. The same type of deformation is also observed in skarn minerals closely associated with the ore at the Madem Lakos deposit.

The main ore mineral paragenesis at Olympias regardless of deformation is pyrite, galena, sphalerite, and arsenopyrite with quartz, calcite, and rhodochrosite as gangue minerals.

Lead isotope compositions of deformed or undeformed ore galenas indicate a crustal source and are homogeneous and identical with K feldspar leads from the Stratoni granodiorite and other Tertiary Greek orogenic granites. These data suggest that the source of the ore leads should be sought in the source of the magmas. Moreover, the crustal affinity and homogeneity of the studied lead isotopes are in agreement with the crustal component contributing to the Tertiary granite formation, even though leaching of lead from crustal rocks cannot be completely disregarded.

The narrow range of sulfur isotope ratios in all the sulfides, and their proximity to 0 per mil, combined with the relatively limited occurrence of sulfates (e.g., gypsum) at Madem Lakos may suggest the combined effects of high reduced/oxidized sulfur species ratios, relatively high temperature, and small $\delta^{34}\text{S}_{\text{initial}}-\delta^{34}\text{S}_{\text{H}_2\text{S}}$ values, thus suggesting an igneous origin for the sulfur.

Fluid inclusion studies in ore-related quartz from Olympias have shown that both deformed and undeformed ore varieties have formed by the same H₂O-dominated CO₂-bearing fluids of low to medium salinity, at temperatures of 300° to 400°C, and pressures of 300 to 800 bars. Preliminary fluid inclusion data from Madem Lakos show higher homogenization temperatures up to 480°C and complex salt (NaCl-KCl-CaCl₂) contents.

Oxygen isotope analyses of ore-related quartz and calcites combined with thermometric data from fluid inclusions and arsenopyrite composition suggest that the mineralizing fluids were of either magmatic or metamorphic derivation with late involvement of meteoric waters. Oxygen and carbon isotope analyses from upper marble-, host marble- to ore-related calcites show a depletion primarily of oxygen indicating an isotopic exchange with infiltrating H₂O-dominated mineralizing fluids. This depletion is correlatable with the degree of hydrothermal alteration expressed by enrichment in the ore host marble compared with the upper marble horizon.

Bulk ore compositions in terms of Cu-Pb-Zn, Cu-Pb+Zn-Ag×10³ ternary diagrams, and Pb-Ag relations show a similarity of the Olympias with the skarn replacement ore type, rather than with the sediment-hosted or the volcanogenic Pb-Zn types. These data, together with data from mineralogical and fluid inclusion studies, suggest that Olympias is predominantly a distal (replacement), whereas Madem Lakos is a proximal (skarn) phase of a skarn replacement ore system.

Therefore, our preferred interpretation is that both deformed and undeformed ore varieties at the Olympias (also presumably at Madem Lakos) deposit formed during the same Tertiary skarn replacement metallogenetic event from fluids of primarily magmatic derivation through reaction with the host marbles at low pressures (300–800 bars) and relatively high temperatures (300°–400°C).

Introduction

THE Olympias, Madem Lakos, and Mavres Petres Pb-Zn(Au,Ag) sulfide ore deposits occur in the Kerdilia Formation of the Paleozoic or older Servo-Macedonian massif (Kockel et al., 1977), eastern Chalkidiki Peninsula, Northern Greece (Figure 1) and are the only producers of Pb, Zn, Cu, and Au-bearing pyrite concentrates in the country.

In 1986 the ore reserves of the Olympias deposit were estimated to be 16 million metric tons averaging 3.3 percent Pb, 5 percent Zn, 120 g/metric ton Ag, and 5.5 g/metric ton Au, whereas those of Madem Lakos, together with Mavres Petres, were estimated at 4.7 million metric tons averaging 4 percent Pb, 4 percent Zn, 110 g/metric ton Ag, and 1.5 g/metric ton Au. Since the first descriptions by Neubauer (1957), Nicolaou (1964, 1971), and Nicolaou and Kokonis (1980), no other work has been published on these deposits. This is the first published study that combines field evidence, mineralogical, geochemical, fluid inclusion, and stable and radiogenic isotope data, primarily from the Olympias deposit in an attempt to determine the ore genesis.

Regional Geology

Lithostratigraphy of the Kerdilia Formation

The Kerdilia Formation constitutes the eastern part of the Paleozoic or older (Kockel et al., 1977) Servo-Macedonian massif. The western part is the tectonically overlying (Stratoni-Varvara fault) Vertiskos Formation (Fig. 1).

The Kerdilia Formation is a heterogeneous assemblage of migmatitized biotite, hornblende-biotite,

hornblende gneisses and also amphibolites and marbles. These rocks have been intruded in Tertiary by the Stratoni granodiorite (Fig. 1), calc-alkaline lamprophyre dikes, and a network of tonalitic-granitic pegmatites-aplites. The latter rocks are more abundant between the Stavros-Stratoni area (Fig. 1).

The lithostratigraphy of the Kerdilia Formation (Kockel et al., 1977) can be considered only as a first approximation as the rocks have been affected by polyphase deformation and metamorphism, igneous activity, and pyrometasomatism. The predominant lithologies from east (lower parts) to west (higher parts) and their approximate thickness are as follows: biotite gneiss: 700 m, lower marble: 0 to 150 m, biotite gneiss: 100 m, intermediate marble: 10 to 200 m, biotite gneiss 70 to 1,000 m, and upper marble: 30 to 300 m.

These rocks are variably intercalated with hornblende-biotite gneisses, amphibolites, and plagioclase-microcline gneisses.

Marbles: Three main grayish white to white marble horizons intercalated with the gneisses are present in the Kerdilia Formation: (1) an upper horizon to the west that also marks the tectonic contact with the Vertiskos Formation, (2) an intermediate horizon, and (3) a lower horizon to the east that is known to host the main Pb-Zn(Au,Ag) massive sulfide orebodies (Fig. 1). The mineralogy of the former two marbles consists of calcite, quartz, muscovite, chlorite, phlogopite, and minor graphite, whereas that of the lower marble horizon is calcite, dolomite, rhodochrosite, quartz, chlorite, tremolite, phlogopite, diopside, actinolite, clinoclone, skapolite, and graphite (Kalogeropoulos et al., 1989a). Andradite garnet and epidote, although

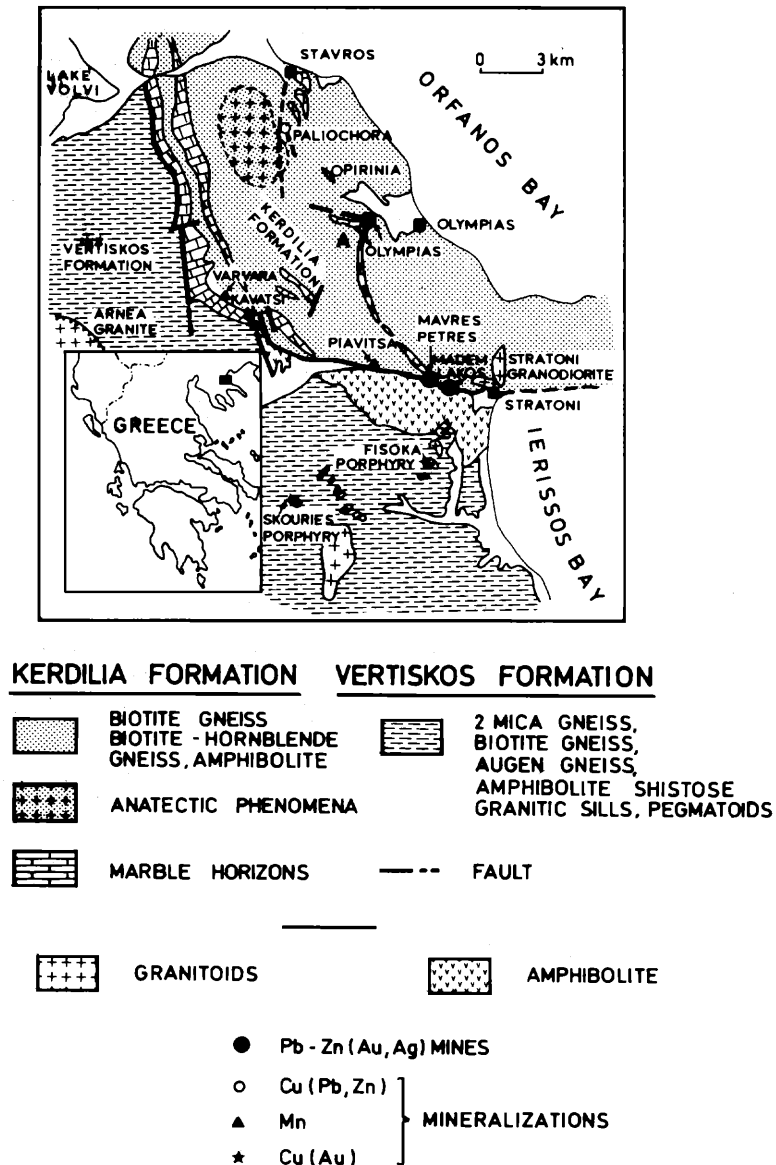


FIG. 1. Simplified geologic map of eastern Chalkidiki, northern Greece, after Kockel et al. (1977).

commonly observed in the Madem Lakos host marble, are lacking at Olympias. Tremolite, diopside, skapolite, and phlogopite occur in close association with pegmatite-aplite dikes. Diopside, tremolite, and phlogopite are hydrothermally altered (Kalogeropoulos et al., 1989a). Moreover, the lower marble horizon compared with the other two shows intense deformation and also higher frequency of granoblastic textures. Graphite in the marbles is considered to be the metamorphic product of carbonaceous matter.

Application of carbon geothermometry on three calcite-graphite pairs ($\delta^{13}\text{C}$, PDB values are 2.2 to -5.0, 0.5 to -3.4, -0.22 to -4.7, respectively), using

the fractionation equation of Friedman and O'Neil (1977), gives only one equilibrium temperature of 657°C which lies within the temperature range of regional metamorphism (see section on biotite gneiss). The disequilibrium state which resulted from the other two pairs is most likely due to fluid-marble interaction (E. Simos, 1988, pers. commun.).

The lower marble horizon shows a statistically significant (95% *p*) increase in the concentrations of MgO, SiO₂, U, Ba, As, Sb, Cu, Mo, Zn, Ni, and Ce and a decrease in CaO relative to the intermediate and upper marble horizons. (Kalogeropoulos et al., 1989a).

Biotite gneiss: Biotite gneiss is the most abundant rock type of the Kerdilia Formation. It varies from medium to coarse grained, banded or foliated, to extremely schistose. Plagioclase (modal 44%), quartz (27%), biotite (20%), garnet (4%), microcline, epidote, sphene, apatite, and zircon constitute its metamorphic mineralogy. The conditions of regional metamorphism as deduced from the application of pertinent geothermometers and barometers are 4 to 9 kbars pressure and 540° to 670°C temperature. (Kalogeropoulos et al., 1989b).

Hornblende-biotite gneiss, amphibolites, plagioclase-microcline gneiss: These rock types are intercalated with the biotite gneisses and the marbles. They bear textures and structures similar to those present in the biotite gneisses and consist of the following respective metamorphic main mineralogies (Nicolaou, 1960; Dimitriadis, 1974; Kockel et al., 1977): plagioclase (44%), hornblende (19%), biotite (16%), quartz (13%), epidote, garnet, sphene; hornblende (54%), plagioclase (39%), biotite (2%), clinopyroxene, epidote, sphene; plagioclase (36%), quartz (29%), microcline (25%), biotite (8%), and muscovite (2%).

Protoliths: On the basis of field relations between the marbles and the other lithologies of the Kerdilia Formation, together with major element data, and the scanty occurrence of graphite in the gneisses and the amphibolites, Dimitriadis (1974) suggests a graywacke protolith for the biotite gneisses and a sedi-

mentary precursor of marl composition for the amphibolites. The same view is also shared by Kockel et al. (1977). However, Fournaraki (1981) in a mineralogical and geochemical study of the Servo-Macedonian amphibolites suggests an igneous origin for these amphibolites. Moreover, application of several criteria (De la Roche, 1968; Garrels and Mackenzie, 1971; Shaw, 1972; Van de Kamp et al., 1976) that discriminate between sedimentary and igneous protoliths on recently obtained chemical data from the Kerdilia gneisses and amphibolites (IGME, unpub. data) indicate a graywacke parent for some biotite gneisses. The rest of the biotite, biotite-hornblende gneisses, the leucocratic gneisses, and the amphibolites have protoliths of igneous origin. In addition, trace element data of the amphibolites point to a sub-alkaline basaltic-basaltic-andesitic composition of tholeiitic affinity with midocean ridge basaltlike characteristics (IGME, unpub. data).

Deformation and metamorphism

Dixon and Dimitriadis (1985) in a study of the metamorphosed ophiolitic rocks from the Servo-Macedonian massif, in combination with additional geologic information (Kockel et al., 1977) (i.e., Arnea granite, Fig. 1), and isotopic ages, concluded that the central and eastern parts of the Servo-Macedonian massif were affected by an amphibolite facies regional metamorphic and deformation event in the Late Ju-

TABLE 1. Deformation, Metamorphism, and Probable Age of the Kerdilia Formation of the Servo-Macedonian Massif

Deformation		Metamorphism		Probable age	
1 ¹	2 ²	1	2	1	2
—	D ₁ Residual forms (?) isoclinal	—	M ₁ Eclogite (?)	—	Paleozoic (?)
D ₁ b = 135°–170° Isoclinal, recumbent decimetric-metric scales	D ₂ b = 120° Isoclinal	M ₁ Amphibolite	M ₂ Amphibolite P = 7–8 kbars T = 600°–650°C	Hercynian	Pre-Upper Triassic
D ₂ b = 125°–155° Subisoclinal, tight, asymmetric decimetric-metric scales	D ₃ b = 150° Tight, isoclinal	—	M ₃ Amphibolite P = 5.7 kbars T = 550°–600°C	Upper Jurassic Lower Cretaceous	Middle-Upper Jurassic
D ₃ b = northwest-southeast Open-tight, asymmetric Southeast Megascopic scale	D ₄ b = 180° Tight, isoclinal	—	M ₄ Upper greenschist P = 4–5 kbars T = 500°–550°C	Upper Cretaceous	Lower-Upper Cretaceous
D ₄ b = northwest-southeast Open metric-decametric scales	D ₅ b = 270° Tight-open and/or isoclinal	—	M ₅ Middle-Lower P = 2–3 kbars T = 350°–450°C	Middle Eocene	Eocene- Oligocene
D ₅ b = north-south Kink band	—	—	—	Oligocene	—

1, Patras et al. (1986); 2, Sakelariou (1988)

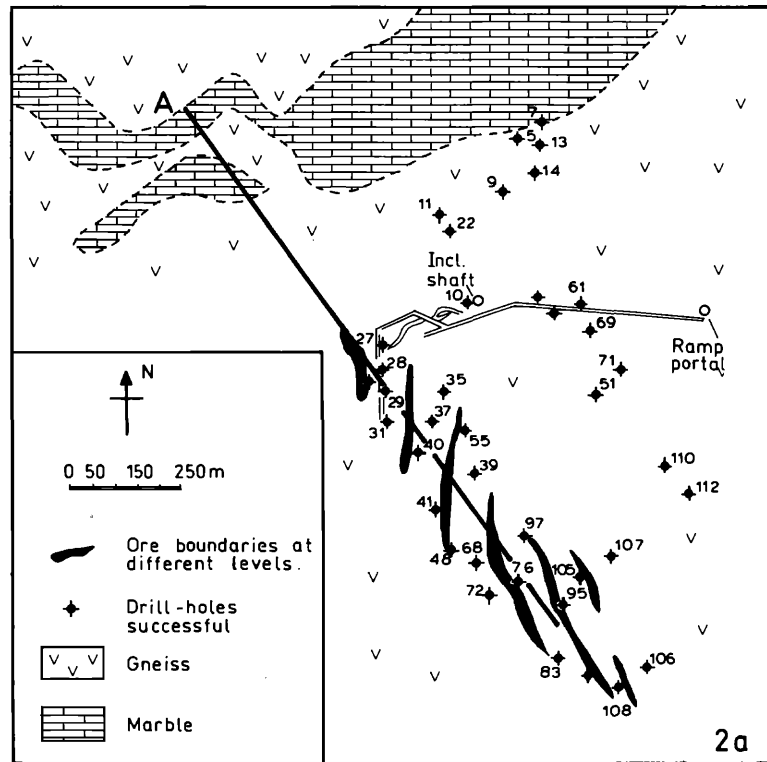


FIG. 2. a. Surface geologic plan of the Olympias mine area. b. Longitudinal geologic section of a. c. Mine cross section showing different levels (Nicolaou and Kokonis, 1980).

rassic-Early Cretaceous (also Papadopoulos, 1982; and Papadopoulos and Kiliadis, 1985).

The Tertiary ages of amphibolites and certain pegmatites, found in the Kerdilia Formation based on K/Ar and Rb/Sr radiometric data in muscovites (Kalogeropoulou and Theodoroudis, 1988), may be explained by delayed uplift of the Kerdilia Formation relative to the Vertiskos Formation.

However, if these metamorphosed ophiolites were Paleotethyan remnants (Sengor et al., 1985) then this amphibolite facies regional metamorphism and deformation event is younger than Early Cretaceous. This event seems to last until early Tertiary in the Kerdilia Formation, culminating to calc-alkaline magmatism at about 50 to 20 Ma (Kalogeropoulou and Theodoroudis, 1988).

The upper time limit of this amphibolite facies regional metamorphism and the associated ductile deformation (tight, isoclinal recumbent folds) in rocks of the Rhodope massif which are similar to those of the Kerdilia Formation is 45 to 50 Ma (Liati, 1986; I. Gerolymatos, 1988, pers. commun.). The results from two recent studies on the deformation and metamorphism of the Servo-Macedonian massif are summarized in Table 1.

The ages assigned to distinct deformation and metamorphism events are not supported by pertinent isotopic evidence, and therefore any further discussion on these results will be premature. However, a point of significance is that even the greenschist facies metamorphism (Table 1) is also characterized by tight isoclinal folds.

Two further points of significance to ore formation are: (1) Certain parts of the Olympias sulfide mineralization are deformed by tight, isoclinal folds; a feature also observed at the Madem Lakos and Mavres Petres deposits. (2) Skarn mineral assemblages produced at the contact of marble with the 29.4-Ma Stratonis granodiorite (Fig. 1) are also similarly deformed by tight isoclinal folds. This deformation has also affected a mafic phase of the granodiorite.

These two points combined with the data referred to above cannot exclude post-Eocene ages for the deformed parts of the sulfide mineralization.

Pegmatites-aplites

A dense network of tonalitic to granitic pegmatites-aplites is found in the area between Stavros and Stratonis villages, in the Kerdilia Formation (Fig. 1). A small proportion of these rocks shows the same char-

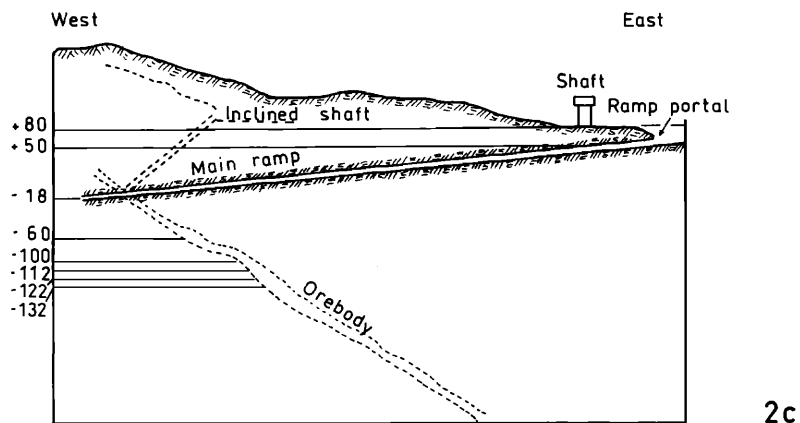
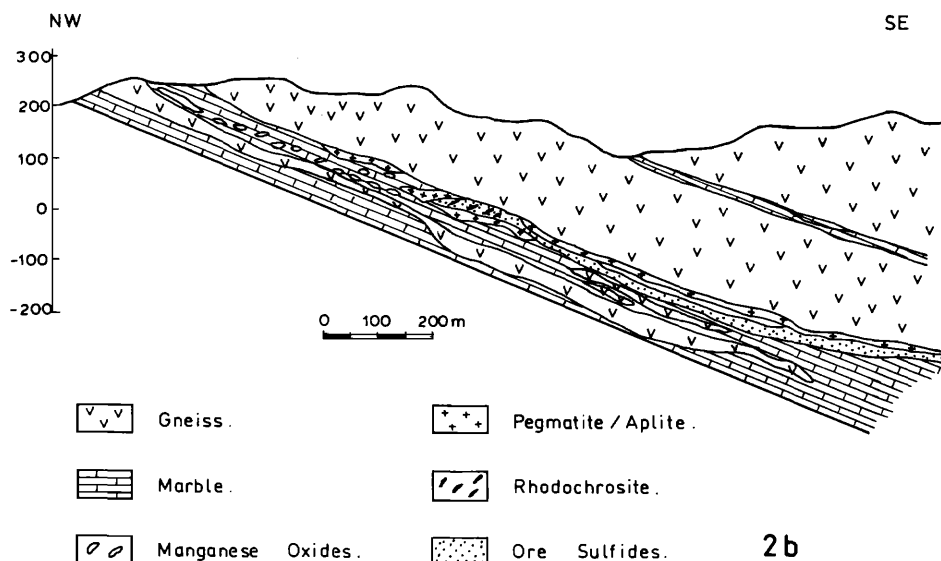


FIG. 2. (Cont.)

acteristics of deformation with the host gneisses and are in thermal equilibrium with them (Dimitriadis, 1974). These pegmatites are considered as products of incipient in situ partial melting (Dimitriadis, 1974; Kalogeropoulos et al., 1989b).

The majority of the pegmatites are, however, in thermal disequilibrium with the intruded lithologies and may occur either as mineralized or barren deformed or nondeformed varieties. Hydrothermal alteration of pegmatites is related to mineralization, thus postdating pegmatite consolidation.

The unaltered pegmatites commonly consist of quartz, K-feldspar, and plagioclase, with biotite, muscovite, garnet, epidote, zircon, apatite, ilmenite, and allanite as accessories. In the altered pegmatites apart from the sulfide veins and disseminations, K-

feldspar is transformed to sericite, plagioclase to carbonate, biotite to chlorite, sphene to rutile, and garnet to biotite, chlorite, and sericite. These pegmatites according to Kalogeropoulos et al. (1989b) are products of anatectic processes that have taken place in deeper parts where pressures and temperatures have exceeded fluid-dominated minimum melt conditions. They have most likely been emplaced as, and consolidated from, a fluid phase at pressures ranging from 0.8 to 2.8 kbars to 3.5 to 5.2 kbars and temperatures ranging from 400° to 500°C. (Kalogeropoulos et al., 1989b).

In addition, the time of the pegmatite-aplite emplacement is considered to span from 50 to 30 Ma (Kalogeropoulos and Theodoroudis, 1988; Kalogeropoulos et al., 1989b).

Stratoni granodiorite

The 29.6 ± 1.4 -Ma (Papadakis, 1971; Altherr et al., 1976; R. Frei, 1988 writ. commun.) Stratoni granitic pluton, located approximately 0.5 km north-northwest of the Stratoni village (Fig. 1), is a magnetic body with a surface outcrop of about 3 km².

This pluton intruded the Kerdilia metamorphics during the late to postdeformational period, along with mineralized and hydrothermally altered peg-

matite-aplite dikes. The primary mineralogy consists of quartz, K-feldspar, plagioclase, biotite, amphibole, clinopyroxene, sphene, and magnetite (Nicolaou, 1960; Kalogeropoulos et al., 1989a). The secondary minerals, produced by hydrothermal alteration, are carbonate, chlorite, sericite, epidote, and pyrite. On the basis of its mineralogy and chemistry, the Stratoni pluton is classified as quartz diorite to granite and is collectively called granodiorite.

The chemistry of this granodiorite is compatible

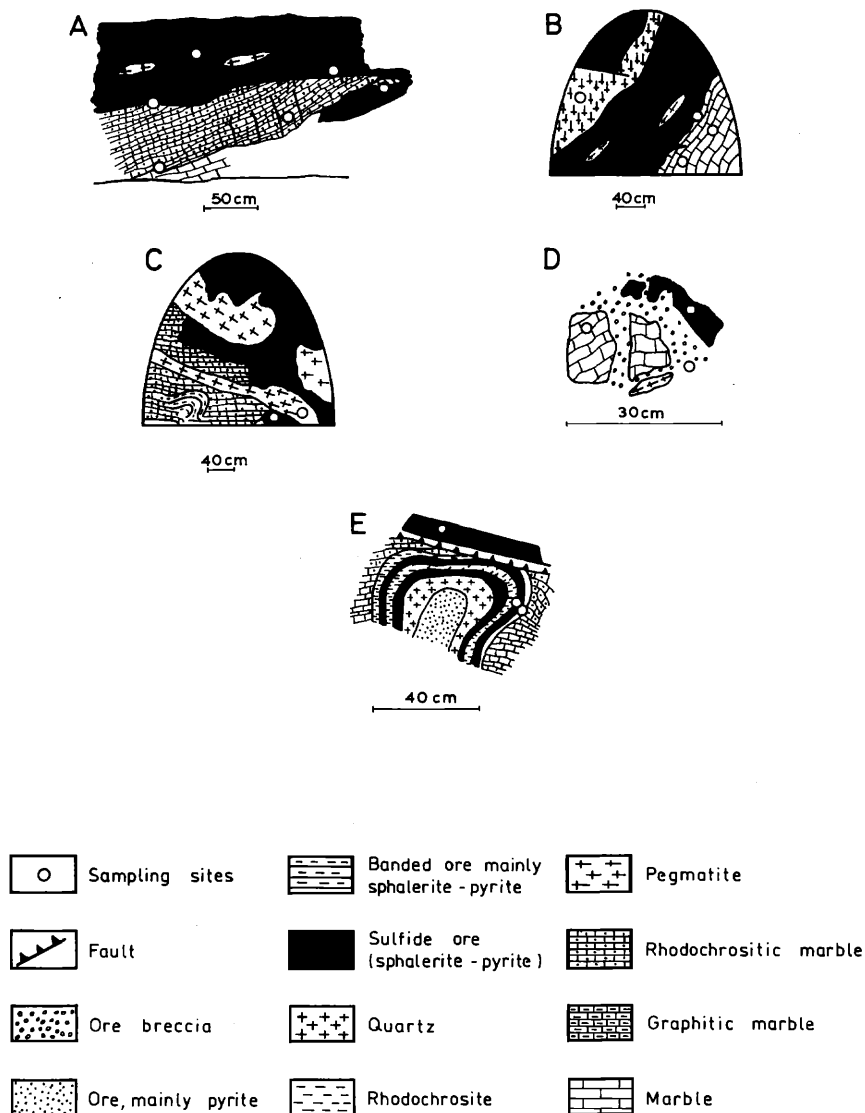


FIG. 3. Mineralization types and relationship to host carbonates and associated pegmatites-aplites, from the Olympias deposit. A. Discordant contact between mineralization and rhodochrositic marble (level -112, looking southwest). B. Concordant contact between mineralization and calcitic marble (level -132, looking southeast). C. Discordant contact between mineralization and rhodochrositic marble crosscut by pegmatite-aplite (level -12, looking northeast). D. Polymictic breccia cemented by pegmatite-aplite with mineralization. E. Concentric ore and gangue deposition within a cavity (level -132, looking southwest).

with formation from a calc-alkaline magma of hybrid nature consisting of predominantly mantle- and also crust-derived components. It contains minor base metal sulfide veins and disseminations and is spatially associated with the Madem Lakos and Mavres Petres Pb-Zn(Au,Ag) sulfide orebodies (Kalogeropoulos et al., 1988a).

The Tertiary magmatism in the eastern Chalkidiki Peninsula is also represented by the Sithonia (38–54 Ma) and Ierissos (42–52 Ma) granodiorites and the Skouries (20 Ma) and Alatina-Fisoka (32 Ma) porphyries (age data from R. Frei, 1988 pers. commun.).

Lamprophyre dikes

Green to grayish-green-grayish-black dikes ranging in thickness from centimeters to tens of meters have been observed at the Olympias and Madem Lakos areas.

These dikes were initially characterized as andesites-dacites (Neubauer, 1956) but later were correctly classified as lamprophyres (Nicolaou, 1960). These lamprophyres crosscut the metamorphics, and also the Stratoni granodiorite, along a northeast-southwest direction (Nicolaou, 1960). The mineralogy consists of plagioclase, green amphibole, phlogopite, biotite, apatite, and quartz phenocrysts, whereas the groundmass is an assemblage of biotite, K-feldspar, and quartz.

Variable degrees of hydrothermal alteration produced carbonate, sericite, rutile, sphene, quartz, and pyrite (Nicolaou, 1960; Kalogeropoulos et al., 1988b). On the basis of their mineralogy and chemistry they can be classified as minettes. An intensely altered lamprophyre shows a relative enrichment in W, Pb, Zn, and Rb and depletion in La, Ce, Ba, Li, U, Sr, Nb, Y, Ni, and Cr (Kalogeropoulos et al., 1988b).

There is a general agreement today that the lamprophyres: (1) are rocks originating from melts of mantle derivation with or without contamination from crustal rocks (Bachinski and Scott, 1979; Rock, 1984; McNeil and Kerrich, 1985) and, (2) have been emplaced in the form of magmas rich in crystals and a fluid phase or even as hydrothermal fluids (Rock, 1984). Rock et al. (1987) consider that there is a close relationship among calc-alkaline lamprophyres, calc-alkaline intrusions, and gold mineralization.

Structural pattern and control of mineralization

Landsat thematic mapper imagery studies combined with photogeology (Tsombos, 1988), heliborne electromagnetic, KIU studies radiometric (Tsombos and Karmis, 1988) and field observations in the eastern Chalkidiki Peninsula revealed three main linear directions trending east-northeast-south-southwest (70°–80°), southeast-northwest (120°–130°), and

north-south, respectively, and a subordinate east-west one. This structural pattern, also found to persist in the Tertiary basins, indicates that it is either a reactivation of basement fractures or Tertiary structures affecting all units present in the Servo-Macedonian massif.

The regional structural control of the major mineralizations such as the Pb-Zn(Au,Ag) massive sulfides, the Mn (Fe) oxides, and the porphyry Cu (Au) is similar to the orientations of the linears deduced from the studies referred to above (Fig. 1 and also P. Tsombos and S. I. Kalogeropoulos, unpub. data).

Olympias Ore Deposit

The Olympias ore deposit, which forms the main subject of this study, is generally strata bound and in

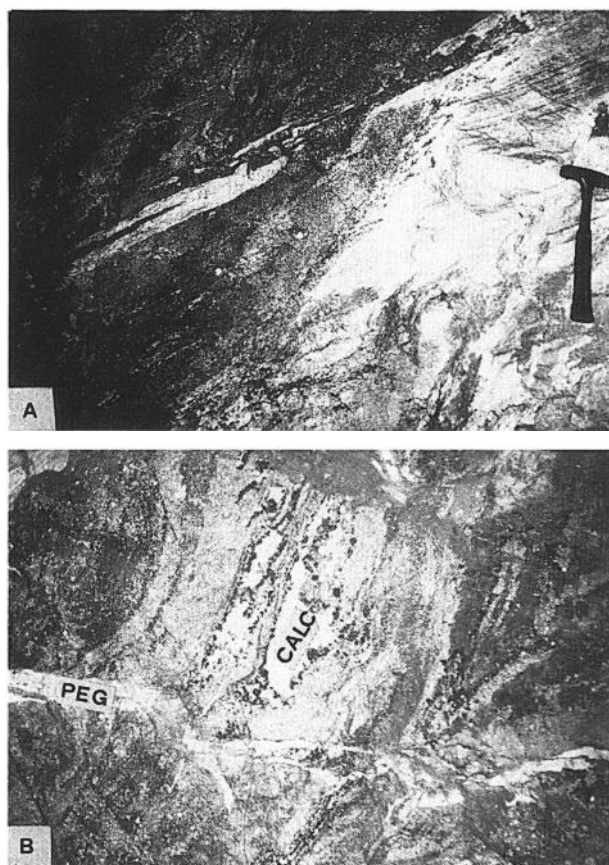


FIG. 4. Mineralization types and relationship to host carbonates and associated pegmatites-aplites, from the Olympias deposit. A. Discordant contact between mineralization and calcitic marble. Note a whitish zone at the contact representing a reaction front. Also note the preserved foliation of the marble within the mineralization. B. Banded ore associated with deformed pegmatite-aplite (PEG). Also shown are cavities filled with calcite (CALC) and mineralization.

places stratiform. It develops along the upper contact of the lower marble horizon with the overlying biotite gneiss and within the marble. However, fault-controlled mineralization has been observed at the Olympias mine at local and regional scales (Kalogeropoulos et al., 1987; Tsombos and Karmis, 1988). The orebody strikes northeast for 1,500 m, dips 30° to 35° southeast to a depth of at least 300 m, and has an average thickness of 12 m (Nicolaou and Kokonis, 1980; Fig. 2a, b, c).

The Madem Lakos and Mavres Petres orebodies occur near or within the Straton-Varvara fault which also marks the tectonic contact between the Kerdilia and Vertiskos Formations (Nicolaou, 1960; Kockel et al., 1977; Tsombos, 1988). The former develops along the marble-biotite gneiss contact, whereas the latter

develops along the biotite gneiss amphibolite tectonic contact. (Fig. 1).

Relationship of ore and host rock

The host rock is white calcitic and rhodochrosite-, and/or Mn calcite-bearing pink rhodochrositic marble (Fig. 3E). The two Mn carbonate minerals also occur early in the ore paragenesis (Fig. 3E). The transition from white to pink marble appears progressive and is characterized by an increase in manganese content accompanying the color change (Kalogeropoulos et al., 1987). The contact of the host marble with the sulfide ore is sharp and concordant (Fig. 3B), or discordant (Figs. 3A, C, E, and 4A). The host marble is characterized by a reaction zone of several tens of centimeters, along the contact with the ore, pro-

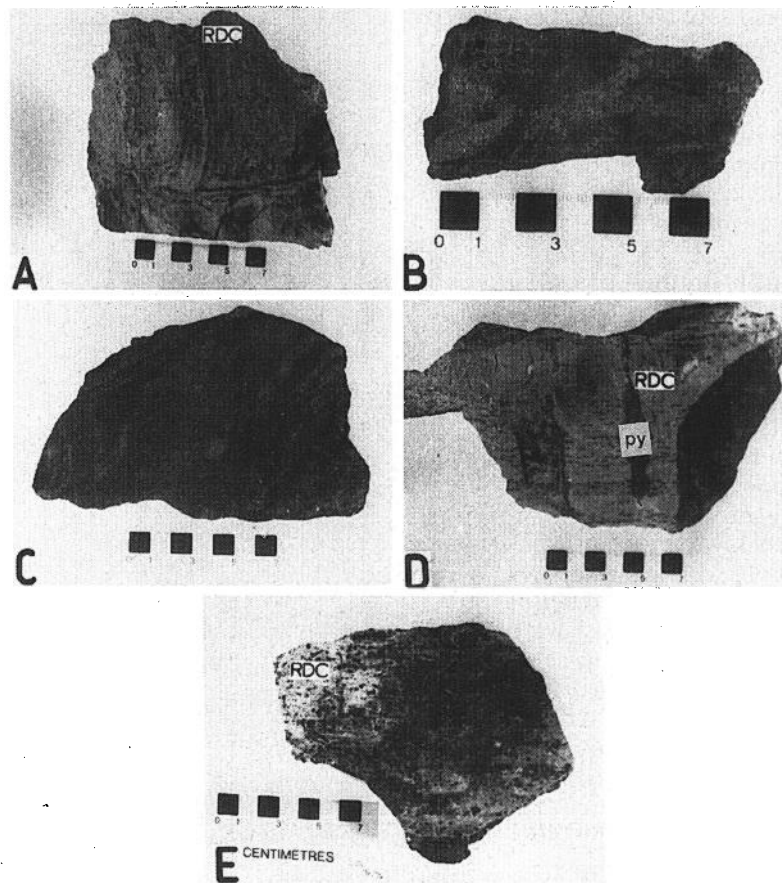


FIG. 5. Forms of mineralization from the Olympias deposit. A. Cavity filling with rhodochrosite (RDC). Note the different orientation of the various minerals. B. Cavity filling with sulfide ore. C. Massive banded ore from a cavity. Note the different orientation of the bands. D. Filling of structural discontinuities mainly with pyrite (py) as well as other ore and gangue minerals. Note that the ore crosscuts the main orientation in the rhodochrositic marble. E. Disseminated ore in rhodochrositic marble.

duced by local scale fluid-rock interaction. This reaction zone bears similar geochemical changes to those deduced by the regional scale lithochemical study referred to earlier in the text (see Marbles section).

Deformed or undeformed varieties of pegmatites-aplites were observed in a mutual crosscutting relationship with the sulfide ores (Figs. 3C, D, and 4B).

Forms of ore mineralization

The ores of Olympias occur in both undeformed and deformed varieties with the former constituting the largest part of the overall sulfide mineralization (also Nicolaou, 1960; Kalogeropoulos et al., 1987; Nebel and Hutchinson, 1988, writ. commun.). It should be noted that the deformed ore at Madem Lakos predates the undeformed ore (Nebel and

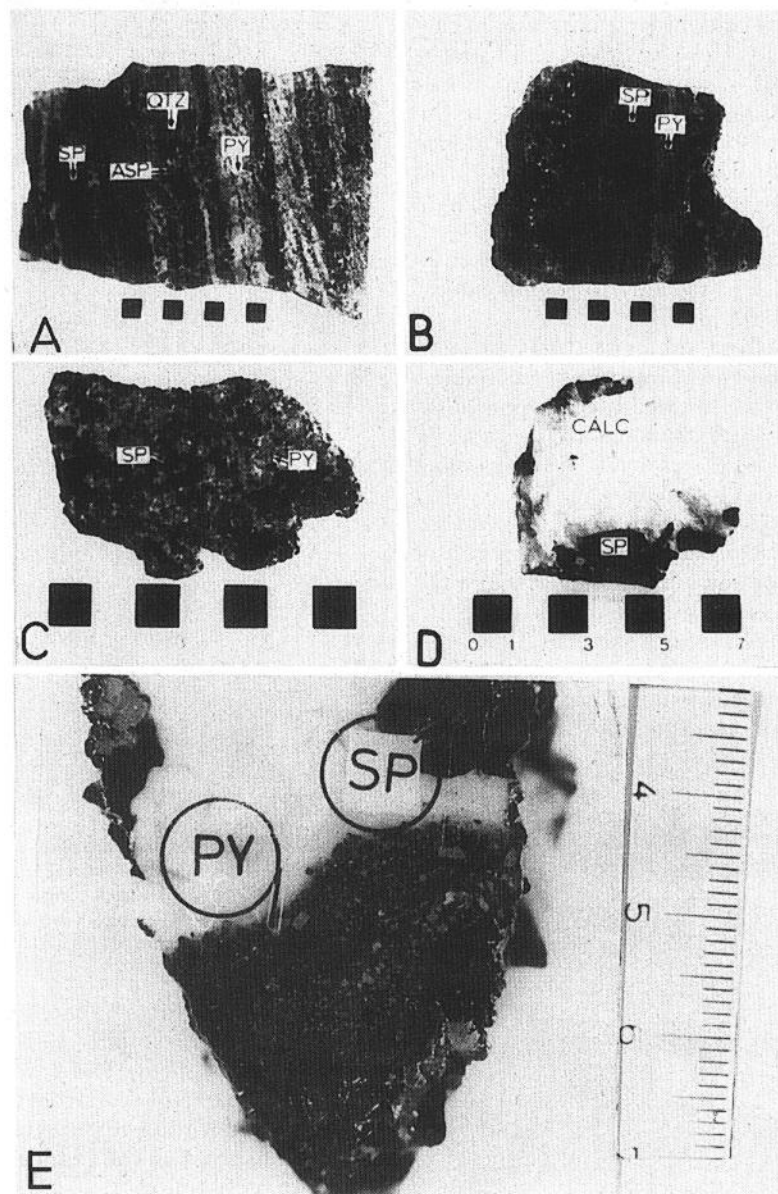


FIG. 6. Forms of mineralization from the Olympias deposit. A. and B. Banded ore consisting of pyrite (PY), sphalerite (SP), quartz (QTZ) and to a lesser extent arsenopyrite (ASP). C. Deformed ore with pyrite (PY) and sphalerite (SP). D. Brecciated sphalerite ore (SP) cemented by calcite (CALC). E. Sphalerite-pyrite (SP-PY) breccia cemented with quartz and calcite.

Hutchinson, 1988, writ. commun.). The deformed ore variety, which is of relatively limited occurrence, is characterized by intense brecciation and also shearing. On the basis of major morphological characteristics, observable at mesoscopic and/or megascopic scale in both ore varieties, the undeformed ore occurs in cavity filling, banded, vein-veinlets, and disseminated forms, whereas the deformed ore appears in brecciated-mylonitized and folded forms, described below:

Cavity filling: This is a concentric deposition of rhodochrosite, sulfides, and minor quartz within cavities in the host marble. These cavities have variable sizes ranging from tens of centimeters to tens of meters. The sequence of deposition from marble to the cavity center is either rhodochrosite to sulfide or vice versa. (Fig. 5A and B). On a megascopic scale, this sequential deposition may eventually result in a banded massive ore variety. (Fig. 5C).

Banded: This consists of alternating bands rich in massive sphalerite, pyrite, arsenopyrite, minor galena, and quartz. (Figs. 5C, 6A and B).

Veins-veinlets: Pyrites, sphalerite, galena, and other sulfides are commonly filling, along with quartz, faults, and fractures in the host marble-forming veins, veinlets or dikes (Fig. 5D). Disseminated sulfides in the host marble (Fig. 5E) also occur accompanying the other forms of undeformed ore.

Brecciated-mylonitized: Some parts of veins or banded ore are brecciated and occur in the form of monomictic (Fig. 6E) or polymictic breccias (Fig. 6D). In addition mylonitic varieties of banded massive ore showing blastomylonitic textures have also been observed (Fig. 6C).

Folded: In certain cases banded ore shows characteristics of ductile deformation indicated by tight,

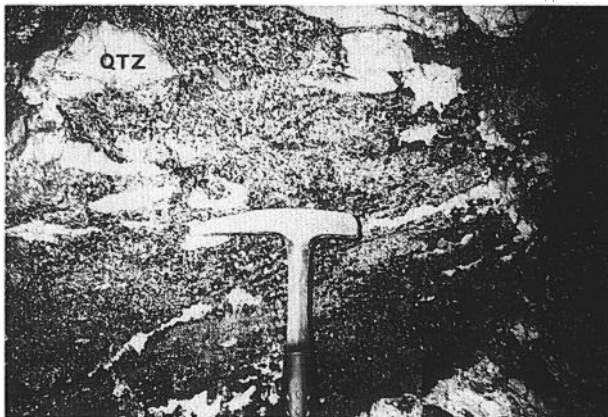


FIG. 7. Deformed banded ore. Note the shear type of deformation exhibited by the enclosed quartz (QTZ) (level -112, looking south).

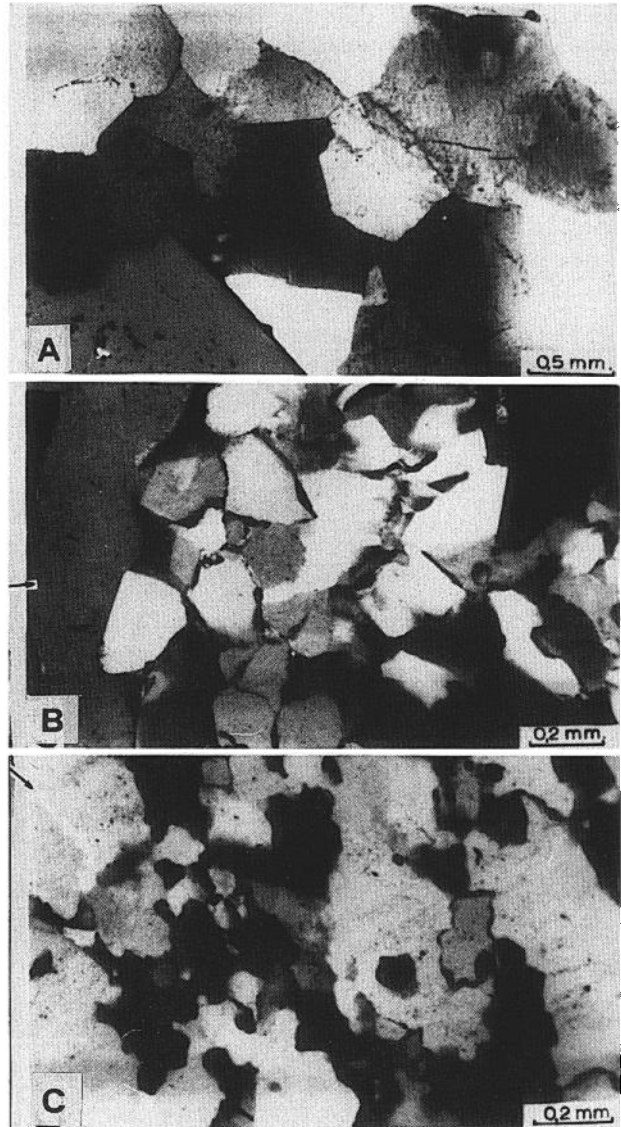


FIG. 8. Textural comparison of quartz from deformed and undeformed mineralization. A. Quartz from undeformed cavity filling ore. Note the triple points. B. Sutured texture of quartz from deformed ore. C. Quartz from deformed ore, texture is similar to B with added deformation.

isoclinally folded quartz bands (Fig. 7). These folds have a general strike of b axes 30° northwest and a plunge of 10° north. The evidence of such deformation is also deciphered from ore microscopic studies. Recrystallization textures and brittle fracturing are also observed in the deformed ore (see also Ore Mineralogy section).

Ore Mineralogy and Mineral Chemistry

The Olympias deposit has a relatively simple sulfide mineral assemblage of pyrite, sphalerite, galena, and

arsenopyrite which forms the bulk of the sulfide material, with subordinate chalcopyrite, tetrahedrite, bournonite, bournonite, pyrrotite, marcasite, geochronite, enargite, graphite, and native gold. Gangue minerals include quartz, rhodochrosite, and calcite (Nicolaou, 1964; Nicolaou and Kokonis, 1980; Kalogeropoulos and Economou, 1987). The major ore sulfide minerals at the Madem Lakos and Mavres Petres deposits are pyrite, sphalerite, arsenopyrite, and chalcopyrite. Other ore zone minerals include tennantite, bournonite, pyrrotite, marcasite, bournonite, cubanite, chalcocite, covellite, magnetite, hematite, graphite, native gold, garnet, and epidote. The gangue minerals are calcite, quartz, and rhodochrosite.

Gold and graphite in all mines occur as inclusions in pyrite and/or arsenopyrite and in sulfides and/or gangue, respectively (Nicolaou, 1964). Ore textures

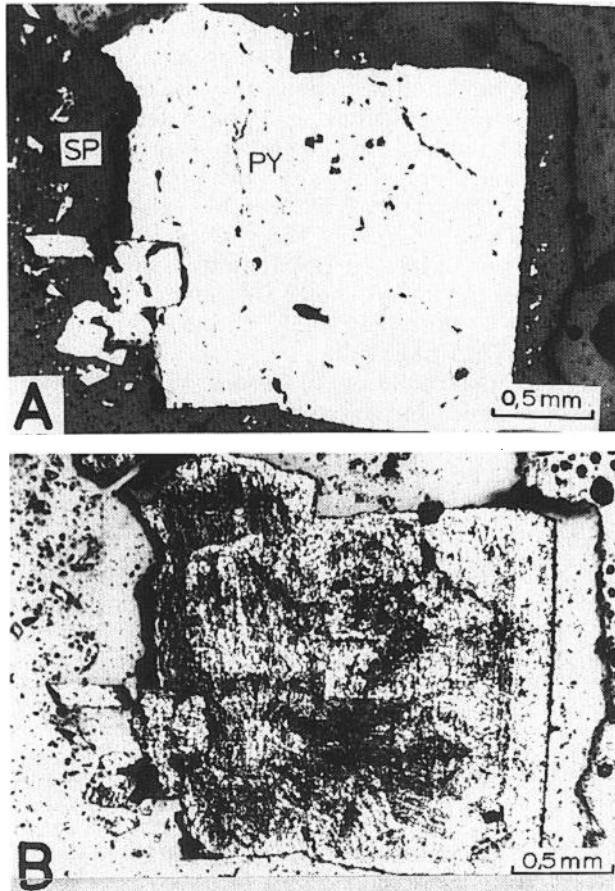


FIG. 9. Photomicrograph of idiomorphic crystal of pyrite (PY) within sphalerite (SP). A. Idiomorphic crystal of pyrite (PY) in reflected light (parallel nichols). B. Growth zoning and complex deposition of the same crystal as in A, after etching with 1NKMnO₄ + 2 percent/vol H₂SO₄.

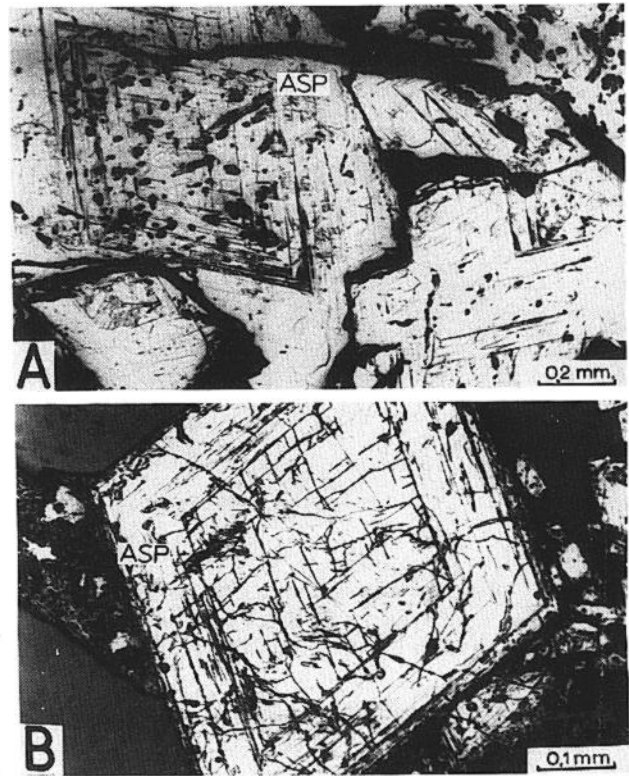


FIG. 10. A and B. Photomicrographs of arsenopyrite (ASP) after etching with 1N KMnO₄ + 2 percent/vol H₂SO₄. Growth zoning of arsenopyrite from undeformed A and deformed B ore. Note the intense cataclasis of B.

include recrystallization, replacement, and probably exsolution (Nicolaou, 1964; Kalogeropoulos and Economou, 1987). The following detailed textural and mineral chemistry data are from Olympias, unless noted otherwise.

Quartz

Quartz is one of the major gangue minerals intimately associated with the sulfide ores. Quartz from undeformed sulfide-bearing veins and cavity-filling ore shows no evidence of deformation and the observed triple junctions are interpreted to be the result of hydrothermal recrystallization (Fig. 8A). Contrary to this, quartz from the deformed ore clearly bears evidence of deformation and different stages of recrystallization (Fig. 8B and C).

Pyrite-arsenopyrite

Both pyrite and arsenopyrite occur mainly as coarse, idiomorphic grains. Those from undeformed ore bear evidence of growth zoning (Figs. 9A, B, and 10A) that is also shown by deformed arsenopyrites (Fig. 10B). Recrystallization in pyrites and brittle de-

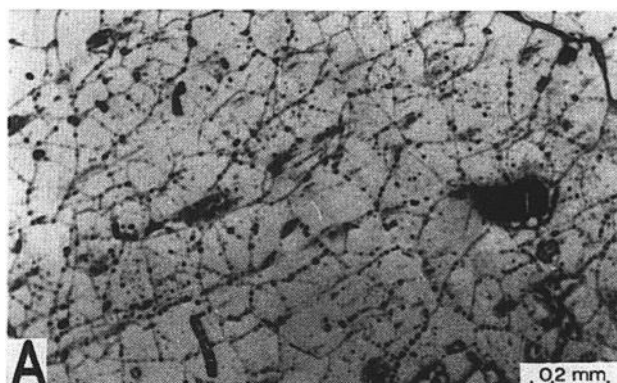


FIG. 11. Photomicrograph of pyrite after etching with 1N KMnO_4 + 2 percent/vol H_2SO_4 . Polycrystalline texture of idiomorphic crystals of pyrite with triple points (granoblastic texture).

formation in arsenopyrite, as well as in pyrite, are observed in deformed ore (Fig. 10B and 11). In addition, the composition of arsenopyrite associated with pyrite in undeformed and deformed ores is the same, indicating similar conditions of formation (Kilias and Kalogeropoulos, 1988).

Sphalerite

Sphalerite exhibits a wide range of textural and chemical variations. These can provide a wealth of information concerning conditions of deposition and subsequent metamorphism of sulfide-bearing rocks and ores (Barton and Toulmin, 1966; Scott and Barnes, 1971; Scott, 1976; Barton, 1978). Sphalerite is a major constituent of the ore sulfide mineral paragenesis of the eastern Chalkidiki sulfide ore deposits. The data presented below are mainly from Kalogeropoulos and Economou (1987) and Kalogeropoulos et al., (1987). Uncovered doubly polished thin sections were used for deciphering textural complexities and chemical variations. The former were studied microscopically before and after etching with 1N KMnO_4 + 2 vol percent H_2SO_4 and the latter were determined

TABLE 2. Compositional Zoning (in wt %) of Undeformed Single Sphalerite Grains from the Olympias Ores and a Veinlet in Altered Pegmatite

	Center <i>n</i> = 5	Intermediate <i>n</i> = 3	Margin <i>n</i> = 3	Sphalerite veinlet in pegmatite		
Zn	54.94	58.50	63.53	60.0	60.9	63.0
Fe	9.88	7.13	2.63	7.5	5.5	4.0
Mn	0.20	0.33	0.23	0.4	0.5	0.6
Cd			0.26			0.1
S	33.20	32.50	33.10	32.2	32.4	32.6
Total	98.22	98.46	99.76	100.1	99.3	100.3

TABLE 3. Electron Microprobe Analyses (in wt %) of Deformed Single Sphalerite Grains from Olympias and Mavres Petres Deposits

	Olympias (OL-122) ¹		Mavres Petres (MP247) ¹		
Zn	59.0	62.0	55.1	56.1	62.7
Fe	6.9	4.1	8.6	7.2	2.6
Mn	0.6	0.6	0.9	0.9	1.1
Cd	0.1	0.1		0.2	0.4
S	33.1	33.0	34.5	34.0	33.8
Total	99.7	99.8	99.1	98.4	100.6

¹ Sample number

by electron microprobe analysis using a JEOL-SUPERPROBE 733. Operating conditions involved: 20 kV excitation voltage, 5nA beam current and 20 s counting time. Mineral standards were used and on-line ZAF corrections were carried out using a PDP-11/04 computer. The data are summarized in Tables 2, 3, and 4.

Cavity and fracture-filling undeformed sphalerites from Olympias, after etching, reveal a texture that consists of polycrystalline aggregates, deduced from the grain boundary touching relationships combined with the linear polysynthetic twins (Fig. 12C, D, and E). These textural features together with the wide chromatic zoning (yellow, brownish yellow, brown, deep brown) and the corresponding variations in the iron content (Tables 2 and 3) are similar to those observed in fracture-controlled and clearly metasomatic Pb-Zn(Au,Ag) sulfide mineralization from the Thermes area, northeastern Greece (Fig. 12A and B; Kalogeropoulos and Arvanitidis, 1988).

Sphalerites from banded deformed ore bear evidence of deformation twinning (Fig. 13A and B) and

TABLE 4. Chemical Composition (in wt %) of Undeformed Sphalerites from the Olympias and Mavres Petres Ore Deposits

	Olympias (51) ¹			Mavres Petres (32) ¹		
	\bar{X}	1σ	Range	\bar{X}	1σ	Range
Zn	56.8	2.3	53.7–63.6	59.8	3.6	53.4–64.8
Fe	8.4	2.2	3.3–10.7	5.4	2.9	1.8–10.4
Mn	0.5	0.3	0.2–1.1	0.8	0.4	0.2–1.8
Cd	0.9	1.1	0.1–2.9	0.3	0.2	0.2–1.0
S	33.4	0.6	32.1–34.4	33.5	0.7	32.0–34.8
Total	100.0			99.8		

¹ Number of analyses

Analyses by electron microprobe (Kalogeropoulos and Economou 1987)

Since sphalerite analyses from Madem Lakos are not representative they are not reported here

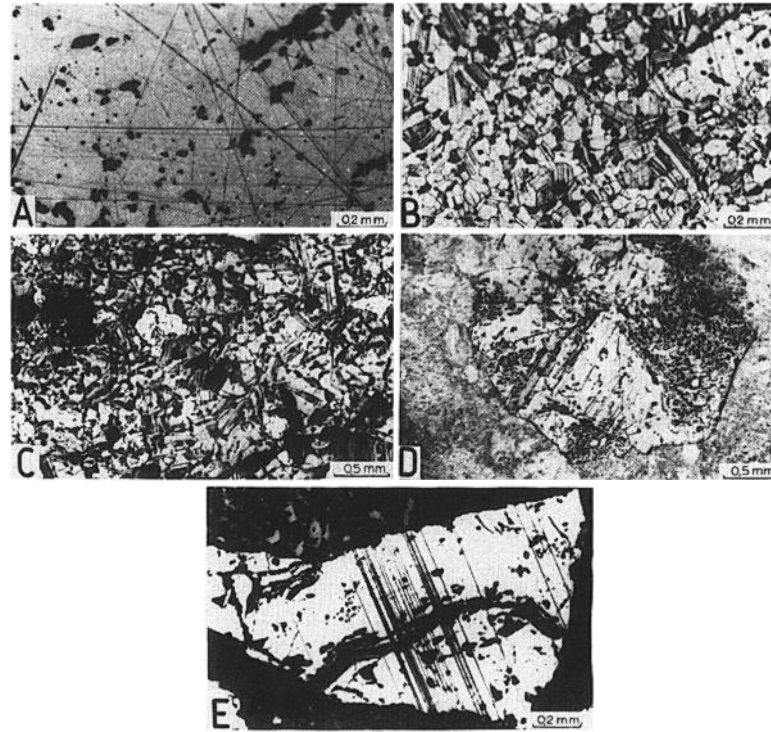


FIG. 12. Photomicrographs of ore textures, Olympias deposit. A. Typical sphalerite from the Olympias deposit and Thermes mineralization, Xanthi, Greece, in reflected light. B and C. A after etching with 1N KMnO_4 + 2 percent/vol H_2SO_4 . Note the polysynthetic twinning. D. Sphalerite from cavity filling ore with polysynthetic twinning and chalcopyrite disease (dotted parts). E. Polysynthetic twinning in sphalerite from structural discontinuity filling ore.

intense mylonitization (Fig. 13C). However, they exhibit chromatic and chemical zoning (Table 3) similar to those seen in the undeformed sphalerites. Moreover, sphalerites from veinlets in an undeformed altered pegmatite at Olympias bear similar characteristics (Table 2) to those described above.

Galena

Galena is generally coarse grained, recrystallized, and is interstitial to sphalerite, pyrite, and/or arsenopyrite. In the deformed ore galena bears evidence of deformation such as bending of cleavages, kink banding, and translation gliding (Fig. 14A and B). However, these features observed in galena are not sufficient to measure the intensity of deformation (Salmon et al., 1974).

Ore Chemistry

The different Pb-Zn sulfide ore deposit types that occur in different environments bear different metal ratios. These ratios are utilized to obtain an independent piece of evidence regarding possible genetic links among them (Sangster and Scott, 1976; Hodgson

and Lydon, 1977; Franklin et al., 1981; Gustafson and Williams, 1981). Since the major constituents of the sulfide ore deposits are the metals Pb, Zn, Cu, Au, and Ag, plots of the relative proportions by weight of Cu-Pb-Zn and $\text{Cu-Pb+Zn-Ag} \times 10^3$ are commonly used for this purpose.

The analyses for Cu, Pb, Zn, and Ag for the Olympias, Madem Lakos, and Mavres Petres deposits are by the Hellenic Company of Chemical Products and Fertilizer S.A. and were performed by conventional AAS. The errors in percent of the analyzed values are: Cu = 10, Pb = 6, Zn = 6, and Ag = 6.

Cu-Pb-Zn and Cu-Pb+Zn-Ag $\times 10^3$ ratios

Figure 15 (A, B, and C) shows plots of the bulk composition of the eastern Chalkidiki Peninsula sulfide ore deposits, regardless of the deformed or undeformed character, in terms of their Cu-Pb-Zn and $\text{Cu-Pb+Zn-Ag} \times 10^3$ contents by weight percent. These data reveal the Pb-Zn nature of the ores as well as their variability of the lead/zinc ratios.

Figure 16 shows the same ternary plots as above, in which the fields of metal ratios for the worldwide

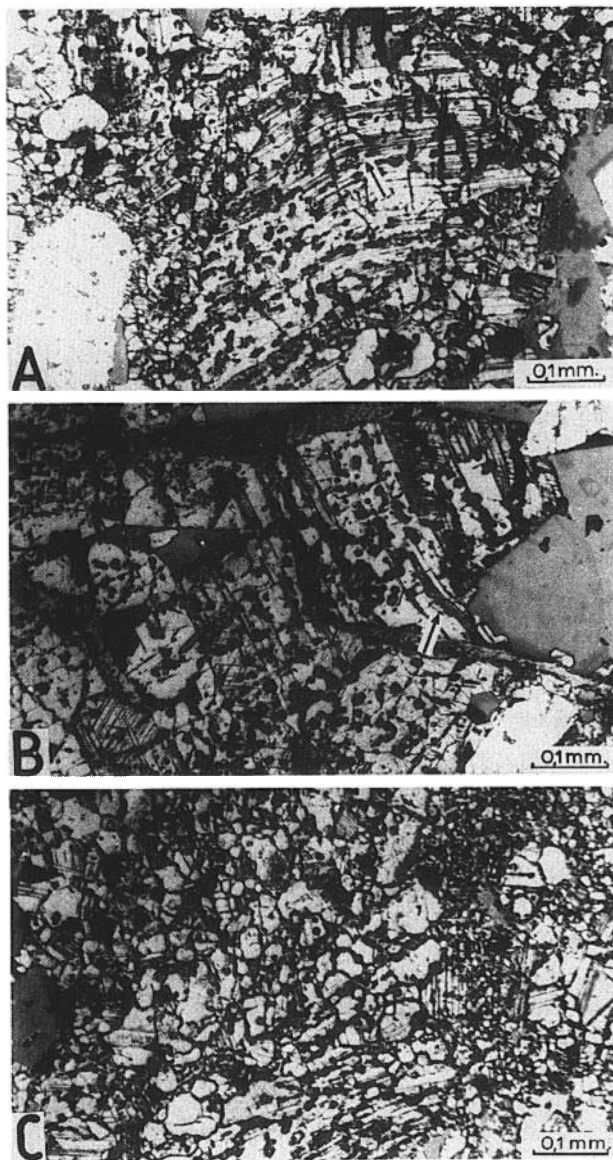


FIG. 13. Photomicrograph of sphalerite from deformed banded ore after etching with 1N KMnO_4 + 2 percent/vol H_2SO_4 . A and B. Sphalerite with deformed twinning arrow shows the ending of the twinning. C. Cataclastic texture of sphalerite.

sediment-hosted, the volcanogenic, and 12 Pb-Zn skarn replacement sulfide ore deposit types are compared with the field occupied by the studied ores. These data suggest a bulk chemical similarity of the eastern Chalkidiki ores with the Pb-Zn sediment-hosted and skarn replacement sulfide ore deposit types. However, a comparison of the Pb-Ag relations between the eastern Chalkidiki sulfide ores on one hand and each one of the Pb-Zn, sediment-hosted, volcanogenic, and skarn replacement sulfide ore deposit types on the other shows a statistically significant

(95% *p*) similarity of the studied ores with the skarn replacement type (Fig. 17).

Fluid Inclusions and Arsenopyrite Composition

Microthermometric studies on primary fluid inclusions in quartz from deformed and undeformed ore samples from the Olympias deposit revealed the presence of three types of inclusions (Kilias and Kalogeropoulos, 1988). Type 1 inclusions contain an H_2O -rich fluid, with no separate CO_2 phase at room temperature, and less than 2.2 mole percent CO_2 as deduced from clathrate formation upon cooling. Total homogenization temperatures and densities range from 240° to 383°C , and 0.6 to 0.85 g/cm^3 , respectively. Type 2 inclusions are CO_2 -rich aqueous fluids with 18 to 33 mole percent CO_2 and contain a separate liquid CO_2 phase. Total homogenization temperatures range from 306° to 383°C and densities from 0.35 to 0.45 g/cm^3 . These two inclusion types occur in both deformed and undeformed ore varieties. Type 3 inclusions, which are rare and limited to the undeformed ore, consist of H_2O -rich solutions with a halite crystal and no detectable carbonic content. These homogenized between 325° to 356°C and have densities up to 1.0 g/cm^3 . Salinities of inclusion types

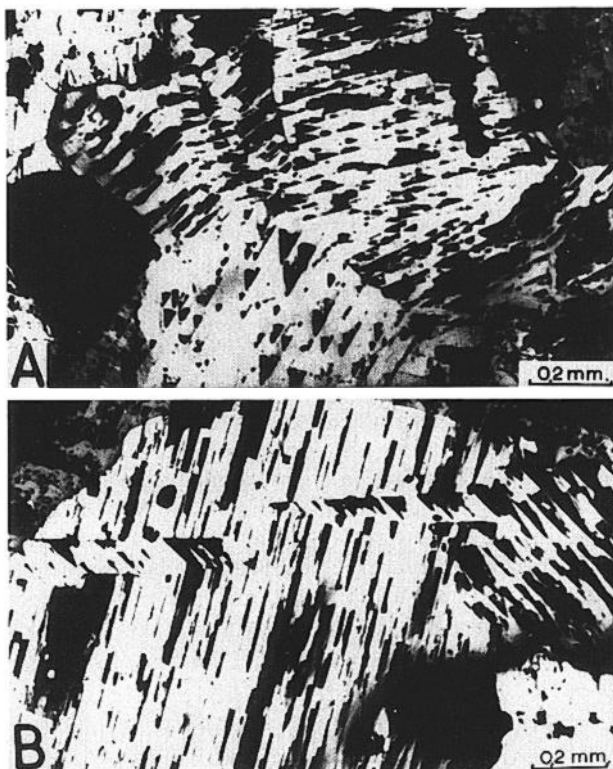


FIG. 14. A and B. Photomicrograph of galena from deformed banded ore after etching. Bent foliation, kink-bands, and translation gliding.

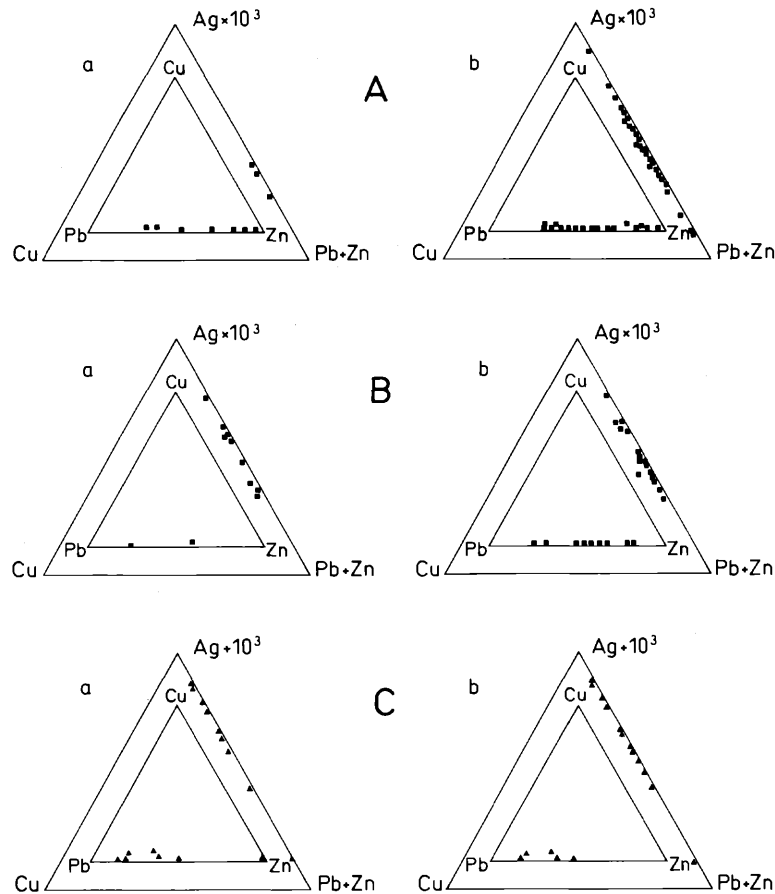


FIG. 15. Ternary diagrams of the ratios of Cu-Pb-Zn (wt %, inside) and Cu-Pb+Zn-Ag $\times 10^3$ (wt %) in ore from single drill holes (a) and a number of drill holes (b) of the Olympias (●) A; Madem Lakos (■) B; and Mavres Petres (▲) C sulfide deposits. Data from the Hellenic Company of Chemical Products and Fertilizers S.A., Greece.

1, 2, and 3 are estimated to be 1 to 17, less than 4, and 28 to 32 equiv wt percent NaCl, respectively.

Densities and isochoric path calculations for coexisting inclusion types 1 and 2 indicate that both the deformed and undeformed ores have formed from similar fluids under similar conditions at temperatures of 300° to 400°C and pressures between 300 to 800 bars.

The arsenic content of arsenopyrites coexisting with pyrite from the same samples studied for fluid inclusions range from 29 to 33 at wt percent (Kiliyas and Kalogeropoulos, 1988) and indicate temperatures broadly similar to those obtained from fluid inclusions. These data suggest that the compositional variation of the Olympias arsenopyrites, and also that of iron content in coexisting sphalerites, reflects primarily temperature variations, as well as minor sulfur fugacity variations, in equilibrium with the bulk arsenopyrite-pyrite-sphalerite ore assemblage.

Sulfur Isotopes

Experimental techniques

The aims of the present study are to (1) determine the first published sulfur isotope compositions of sulfides from the Olympias, Madem Lakos, and Mavres Petres ore deposits; (2) determine, if possible, the equilibration temperatures from coexisting sulfide pairs; and, (3) evaluate the possible sources of sulfur.

The sulfur isotope results are presented in Table 5 and plotted in Figure 18. The $\delta^{34}\text{S}$ values for pyrite, sphalerite, galena, and arsenopyrite from the Olympias deposit are 0.1 to 1.3, 0.0 to 0.7, -1.4 to 0.5, and 0.2 to 0.9 per mil, respectively. The $\delta^{34}\text{S}$ values for pyrite, and sphalerite from the Madem Lakos and Mavres Petres deposits are 0.9 to 2.1 and 0.6 to 1.6 per mil, respectively. No significant variations are observed within the Olympias deposit and between all

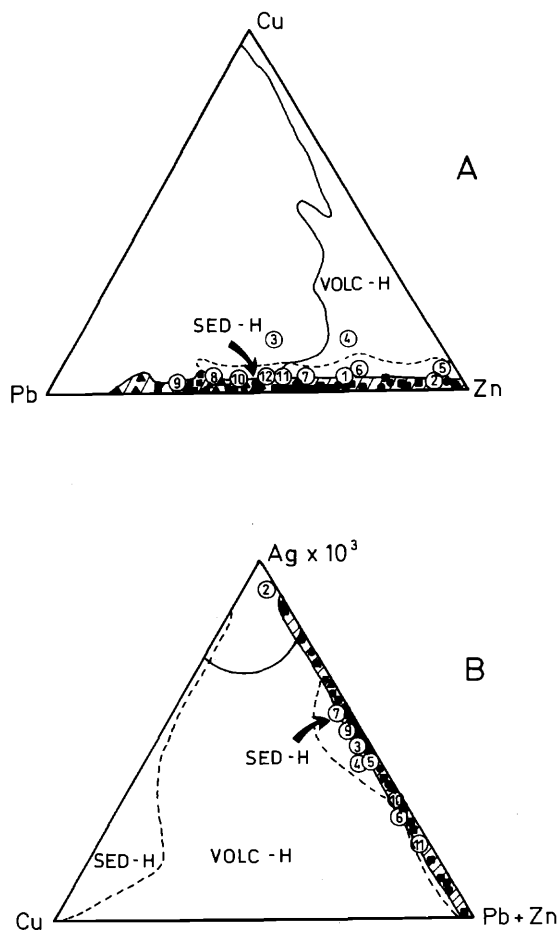


FIG. 16. A. Comparison of the bulk Cu-Pb-Zn, and B. Cu-Pb+Zn-Ag $\times 10^3$ compositions of the sediment-hosted (SED-H) volcanic-hosted (VOLC-H) and skarn Pb-Zn sulfide ore types with the eastern Chalkidiki Peninsula Pb-Zn sulfide ores (hatched area). Data for the former two types in A are from Lydon (1983) and in B are from Gustafson and Williams (1981). Data for skarn-type Pb-Zn sulfide ores shown in circled numbers are from Einaudi et al. (1981). 1 = Ulchiki Peninsula, Korea; 2 = Yeonbwa II, Korea; 3 = Henpaoshan-Sikarg province, China; 4 = Washington Camp, Arizona; 5 = Hanover area, northern Mexico; 6 = Groundhog, northern Mexico; 7 = Frisco, Mexico; 8 = Hildago, Mexico; 9 = Stri Trg, Trepca, Yugoslavia; 10 = Aravaipa, Arizona; 11 = Bluebell, Canada; 12 = Uchucchacwa, Peru. Data for the latter ores are from the Hellenic Company of Chemical Products and Fertilizers S.A., Greece. Symbols are as in Figure 15.

the deposits (Table 5). In addition, the mean $\delta^{34}\text{S}$ value for the sulfides is near 0 per mil.

Fifteen sulfide ore samples were collected from underground working of the Olympias, Madem Lakos, and Mavres Petres mines. Fourteen pyrites, seven sphalerites, four galenas, and two arsenopyrites in various touching relationships were hand separated from the sulfide specimens, with purity better than 97 percent. The 27 sulfide separates were analyzed

for their sulfur isotope signature relative to the Canyon Diablo troilite (CDT) standard, employing standard methods. Analytical uncertainties are ± 0.2 per mil for $\delta^{34}\text{S}$ and ± 0.4 per mil for $\Delta\delta^{34}\text{S}$.

Thermodynamic considerations (Sakai, 1968) and experimental data (Kajiwara and Krouse, 1971) indicate that under isotopic equilibrium conditions the $\delta^{34}\text{S}$ content of the sulfides present should decrease in the order pyrite > sphalerite > galena. All our samples but one follow this trend (Table 5), suggesting a tendency toward equilibrium. The one discrepancy may be attributed to either isotopic disequilibrium or noncontemporaneous precipitation of the coexisting sulfides.

The extent to which isotopic equilibrium has been attained by utilizing the various plotting techniques of Smith et al. (1977, 1978) and Shelton and Rye (1982) cannot be evaluated with only the present data available.

The small difference in $\delta^{34}\text{S}$ values between the pyrite-sphalerite and the pyrite-galena pairs makes them unreliable geothermometers. In addition, the sphalerite-galena pair which exhibits a tendency to equilibrate faster (Kajiwara and Krouse, 1971) and gives temperatures in agreement with those obtained from fluid inclusions in sulfide and associated gangue minerals (Ohmoto and Rye, 1979) is underrepresented in our samples. Therefore, we cannot come to any conclusions as to the extent of equilibrium attained between the coexisting sulfides until additional more detailed sulfur isotope studies are attempted.

The narrow range of sulfur isotope ratios in all the sulfides and their proximity to 0 per mil (Table 5 and Fig. 18), combined with the relatively limited occurrence of sulfates (e.g., gypsum) at Madem Lakos may suggest the combined effects of high reduced/oxidized sulfur species ratios, relatively high temperature, and low $\delta^{34}\text{S}_{\text{initial}} - \delta^{34}\text{S}_{\text{H}_2\text{S}}$ values, thus suggesting an igneous origin for the sulfur (Ohmoto, 1972; Rye and Ohmoto, 1974).

Lead Isotopes

Fourteen galena samples, two from Olympias, nine from Madem Lakos, two from Mavres Petres, and one galena concentrate were analyzed for their Pb isotope composition at the geochemistry laboratories of the University of Amsterdam and the Bureau de Recherches Geologiques et Minières (France). The remaining data are from Chalkias and Vavelidis (1988). The analytical results are presented in Table 6 and plotted in Figures 19, 20, 21, and 22. Figure 19 is part of the respective figures of Doe and Zartman (1979) where they have synthesized the lead isotope characteristics of different geologic environments in their plumbotectonics model. Figures 20 and 21 are the standard $^{207}\text{Pb}/^{204}\text{Pb}$ vs. $^{206}\text{Pb}/^{204}\text{Pb}$ and $^{208}\text{Pb}/$

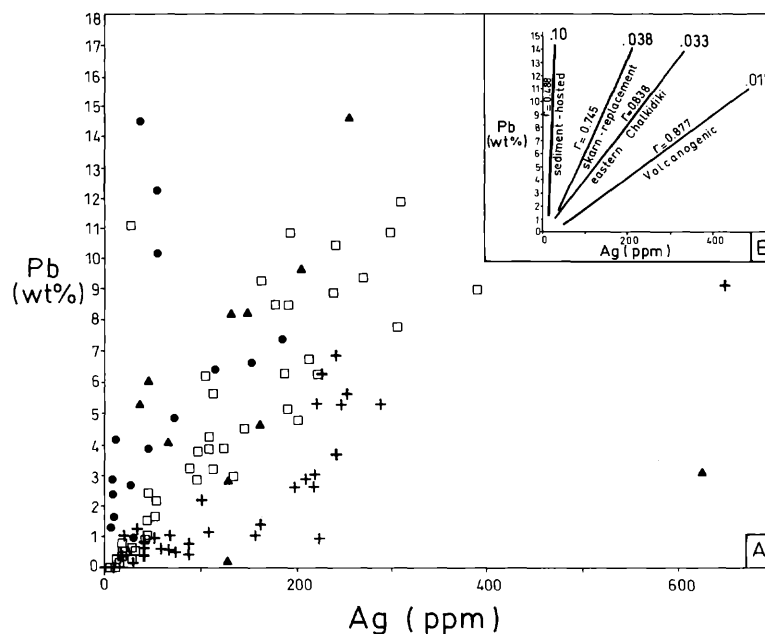


FIG. 17. A. Pb-Ag plot for worldwide distributed sediment-hosted (●), volcanogenic (+), and skarn replacement (▲) Pb-Zn sulfide ore types as compared with the eastern Chalkidiki Peninsula Pb-Zn ores (□). Note the separation of the Chalkidiki ores from the former two ore types and a significant overlapping with the third. Data are from: Lydon (1983); (1977); Einaudi et al. (1981); Hellenic Company of Chemical Products and Fertilizers S.A. B. Best-fit lines, correlation coefficients (r) and slopes (upper end of line) resulted from A data. Two outliers (Ag-rich-Pb-poor samples) from the skarn replacement and three from the sediment-hosted ore types were excluded from the calculations without affecting the conclusions.

²⁰⁴Pb vs. ²⁰⁶Pb/²⁰⁴Pb diagrams, respectively. Stacey and Kramers (1975) reference lead growth curve for average crust with $\mu = 9.74$ and Th/U ratio of 3.70

is shown in both these diagrams. In addition, a lead growth curve with $\mu = 9.94$ and isochron lines starting from 3.7 Ga are also shown in Figure 20. Finally,

TABLE 5. Sulfur Isotope Ratios of Sulfide Minerals from the Eastern Chalkidiki, Pb-Zn (Au, Ag) Deposits

Location and sample no.	Remarks	Sulfide sulfur isotope compositions (CDT in ‰)			
		$\delta^{34}S_{py}$	$\delta^{34}S_{sp}$	$\delta^{34}S_{gn}$	$\delta^{34}S_{asp}$
Olympias orebody					
Rdc 1	Coexisting sulfides	0.4	0.6		
Rdc 2		-0.1			
OL-40	Coexisting sulfides	1.3	0.7		
OL	Coexisting sulfides	0.8		0.5	
OL-68, 1	Coexisting sulfides	1.0	0.0	-1.3	
OL-68, 2	Coexisting sulfides	0.7	0.0		
OL-76, 2	Coexisting sulfides	0.1		-1.4	
OL-76, 2B	Coexisting sulfides	1.0	0.5		
OL-76, 8		0.4			
OL-84, 2	Coexisting sulfides	1.1			0.2
OL-asp					0.9
Madem Lakos (ML) and Mavres Petres (MP) orebodies					
ML 78, 1	Coexisting sulfides	0.9		0.7	
ML 94, 1	Coexisting sulfides	1.1			
MP 247	Coexisting sulfides	1.6	0.6		
MP 160	Coexisting sulfides	2.1	1.6		

Abbreviations: py = pyrite, sp = sphalerite, gn = galena, asp = arsenopyrite, Rdc = rhodochrosite

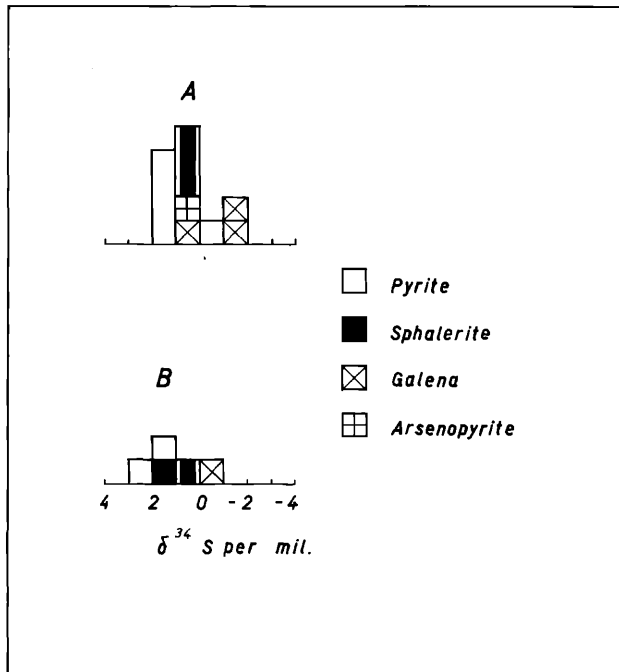


FIG. 18. Sulfur isotope composition of sulfide minerals from the Olympias A and Madem Lakos-Mavres Petres B ore deposits.

Figure 22 is a standard plot where our ore lead isotope data are compared with the K feldspar leads from Tertiary Greek granites (Juteau et al., 1986).

The data from the ore deposits are largely homogeneous exhibiting a small variation outside the two-sigma (2σ) error not correlatable with the deformed and undeformed ore varieties (Table 6). This variation may be attributed to either lead isotope variability in the hydrothermal fluids and/or to small variations of the Th/U ratios in the source materials of the lead (Juteau et al., 1986).

These figures show that the lead compositions plot above the average orogene curve. The μ values range from about 9.70 to 9.97 and the Th/U ratios range from 3.74 to 3.81. All these indicate that the ore lead was derived from preexisting evolved predominantly crustal material. Moreover, the model ages of the galenas are younger than 65 Ma (Fig. 20).

Figure 22 shows that our ore leads are comparable with the K feldspar leads from Tertiary Greek orogenic granites (Juteau et al., 1986, R. Frei, 1989, pers. commun.) suggesting that the source of the ore leads has to be sought in the same rocks as the source of the magma.

Juteau et al. (1986) in a Pb, Sr, and Nd isotope study involving Tertiary Greek granites concluded that they are the products of binary mixtures between a recycled crustal component and a depleted mantle-like component. They have also concluded that large-scale anatexis of the crust is required in order to av-

erage the isotopic signature of heterogeneous terranes. In the first case the mantle-derived component may be represented by differentiated island-arc-type magmas which in turn are mixed with anatectic melts to produce the granites, whereas in the second case the mantle-derived igneous rocks form a part of the crustal segment participating in the anatectic processes. Kalogeropoulos et al. (1988a) concluded, on the basis of geochemistry, that the 29.6 ± 1.4 Ma Stratonis granodiorite is a hybrid product of mantle- and crust-derived components. Also, Dimitriadis (1974) and Kalogeropoulos et al. (1988b) suggest that the majority of the tonalitic-granitic pegmatites-aplites that are abundant in the Kerdilia Formation are products of anatectic processes that have taken place to a significant extent at deeper levels. These data are in agreement with the study of Juteau et al. (1986).

Oxygen and Carbon Isotopes

The values and gradients of oxygen and carbon isotopes of carbonate and silicate minerals in metamor-

TABLE 6. Lead Isotope Ratios of Galenas from the Eastern Chalkidiki Peninsula Pb-Zn (Au, Ag) Sulfide Ore Deposits

Sample no.	Ore deposit	$^{206}\text{Pb}/^{204}\text{Pb}$	$^{207}\text{Pb}/^{204}\text{Pb}$	$^{208}\text{Pb}/^{204}\text{Pb}$
TC40	Olympias	18.780	15.670	38.860
TC39E	Olympias	18.770	15.660	38.820
TC39A-2	Olympias	18.770	15.660	38.800
GRL6	Olympias	18.780	15.680	38.890
GRL7	Olympias	18.790	15.680	38.800
GRL8	Olympias	18.780	15.670	38.820
109B-1	Olympias	18.760	15.660	38.800
-68L	Olympias	18.794	15.678	38.896
G	Olympias	18.794	15.678	38.906
38C	Madem Lakos	18.770	15.660	38.860
GRL1	Madem Lakos	18.780	15.660	38.880
GRL3	Madem Lakos	18.780	15.660	38.910
70L	Madem Lakos	18.778	15.659	38.880
78L	Madem Lakos	18.781	15.660	38.905
G1D	Madem Lakos	18.761	15.662	38.871
G2D	Madem Lakos	18.758	15.644	38.810
G3D	Madem Lakos	18.772	15.651	38.840
G4D	Madem Lakos	18.760	15.645	38.813
P5U	Madem Lakos	18.784	15.659	38.823
Z6U	Madem Lakos	18.798	15.665	38.871
Z7U	Madem Lakos	18.772	15.645	38.816
38A-8	Mavres Petres	18.760	15.620	38.770
GRL4	Mavres Petres	18.810	15.670	38.900
GRL5	Mavres Petres	18.810	15.660	38.900
247L	Mavres Petres	18.807	15.669	38.904
260L	Mavres Petres	18.805	15.665	38.887
	Galena			
Gc	concentrate	18.779	15.671	38.887

Data for samples -68L, 70L, 78L, G1D to Z7U, Z47L, 260L, and G are from this study. The remaining are from Chalkias and Vavelidis (1988)

Abbreviations: D = deformed, U = undeformed, others are undeformed

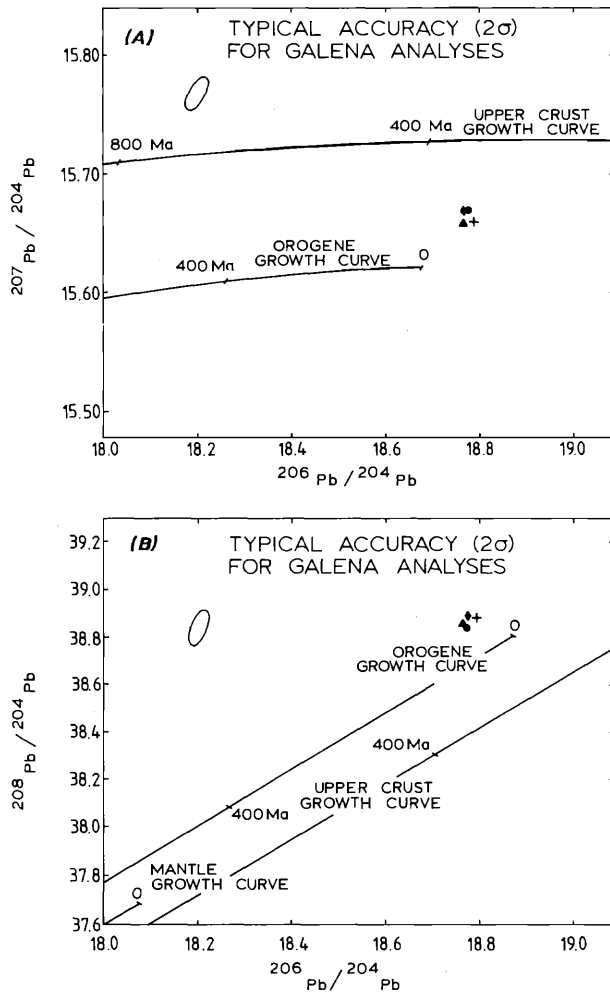


FIG. 19. Plots of $^{207}\text{Pb}/^{204}\text{Pb}$ (A) and $^{208}\text{Pb}/^{204}\text{Pb}$ (B) vs. $^{206}\text{Pb}/^{204}\text{Pb}$ ratios of average galenas from Olympias (●), Madem Lakos (▲), Mavres Petres (+) and concentrate (◆). Orogene, upper crust, and mantle curves are from Doe and Zartman (1979).

phic terranes, especially when mineralization is present, commonly offer a powerful tool for placing constraints on the origin of the mineralizing fluids and the depositional processes. The composition of these isotopes in a marble, as in any other metamorphic rock, depends on (1) the initial isotopic composition of the marble, (2) the decarbonation effects (3) the degree of exchange with infiltrating fluids, and (4) the temperature of exchange.

Thirty six calcite samples from the upper and the lower marble horizons of the Kerdilia Formation as well as 12 ore-related cavity-filling calcites from Olympias and Madem Lakos were analyzed for their ^{18}O and ^{13}C isotopic composition. The analyses were conducted at the laboratories of the Free University of Brussels, Belgium, by P. Pasteels, and the Central Institute of Geology in Copenhagen, Denmark, by

B. Buchardt. In addition, the ^{18}O isotopic composition of 8 ore-related quartz samples was obtained using the analytical facilities of the Central Institute of Geology, Copenhagen, Denmark.

Carbon dioxide was released from calcites by the method of McCrea (1950) and then analyzed for both $\delta^{13}\text{C}$ and $\delta^{18}\text{O}$ on a mass spectrometer. Oxygen was liberated from quartz by reaction with BrF_5 and converted to CO_2 before mass spectrometric analysis according to the method of Clayton and Mayeda (1963). Mass spectrometry was performed on a Variant MAT 250 triple collector instrument.

The carbon isotope values are reported relative to the Pee Dee belemnite (PDB) standard, and the oxygen values relative to the standard mean ocean water (SMOW) standard, in $\delta^{13}\text{C}$ and $\delta^{18}\text{O}$ per mil. Results for both ^{18}O and ^{13}C were reproducible to ± 0.15 per mil and are summarized in Table 7. A plot of the $\delta^{13}\text{C}$ versus $\delta^{18}\text{O}$ values of calcites from the upper and lower marble horizons of the Kerdilia Formation and the ore-related calcites from Olympias and Madem Lakos are shown in Figure 23. Oxygen shows statistically significant depletions from the upper marble calcites to the ore-related calcites, whereas in carbon isotopes the depletion does not seem to be statistically significant.

The amount of oxygen isotope depletion of the hydrothermal calcites and the lower marble calcites relative to unaltered carbonates cannot be the result of isotopic exchange between carbonates and CO_2 produced by batch or Rayleigh decarbonation mechanisms (Kalogeropoulos and Kiliyas, 1988). Instead the oxygen isotope composition of the ore-related carbonates is probably controlled by isotopic exchange with infiltrating H_2O -dominated hydrothermal fluids. This point is further supported by the general correlation of the oxygen isotope depletion with the degree of hydrothermal alteration of the upper and lower marble horizons (Fig. 24).

Oxygen isotope composition of the mineralizing fluids

Using the temperatures obtained from fluid inclusions and arsenopyrite geothermometry studies (Kiliyas and Kalogeropoulos, 1988), the appropriate quartz water and calcite water fractionation equations (Friedman and O'Neil, 1977; Matsuhisa et al., 1979) and the measured $\delta^{18}\text{O}$ mineral values, the oxygen isotope composition of the hydrothermal fluid from which these minerals were precipitated can be calculated assuming equilibrium. The results obtained for a mean fluid inclusion-arsenopyrite temperature at 350°C are shown in Table 8. These oxygen isotope compositions of the fluid are consistent with either magmatic and/or metamorphic solutions. If the mineralizing fluid was magmatic then the variation of the

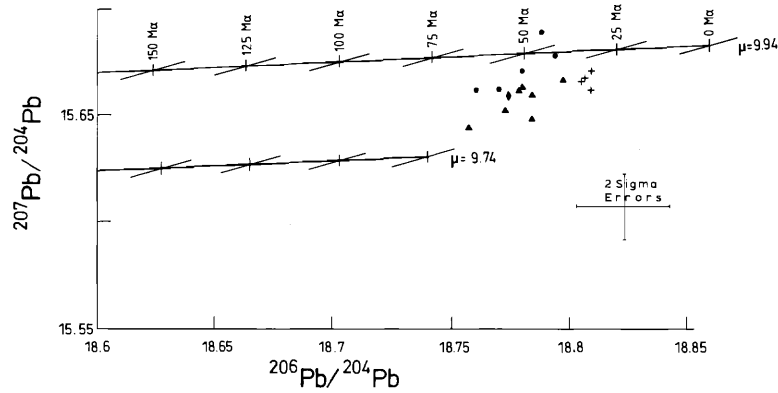


FIG. 20. Plot of $^{207}\text{Pb}/^{204}\text{Pb}$ vs. $^{206}\text{Pb}/^{204}\text{Pb}$ ratios of average galenas from Olympias (●), Madem Lakos (▲), Mavres Petres (+), and concentrate (◆). Lead growth curves for average crust with $\mu = 9.74$, and another with $\mu = 9.94$, with isochron lines starting from 3.7 Ga, are from Stacey and Kramers (1975).

$\delta^{18}\text{O}$ of this fluid from igneous values to over 12 per mil may indicate isotopic exchange with the high $\delta^{18}\text{O}$ of the marble wall rock, whereas the low $\delta^{18}\text{O}$ fluids may suggest contributions from meteoric waters.

Conclusions

The main conclusions of this study are the following:

1. The Kerdilia Formation is a heterogeneous assemblage of migmatitized biotite, hornblende-biotite, hornblende-gneisses, amphibolites, and marbles of probable Paleozoic or older age. A graywacke parent

is indicated for some of the biotite gneisses whereas for the remaining biotite-hornblende gneisses, leucocratic gneisses, and amphibolites an igneous parental origin is suggested. In addition our data on the

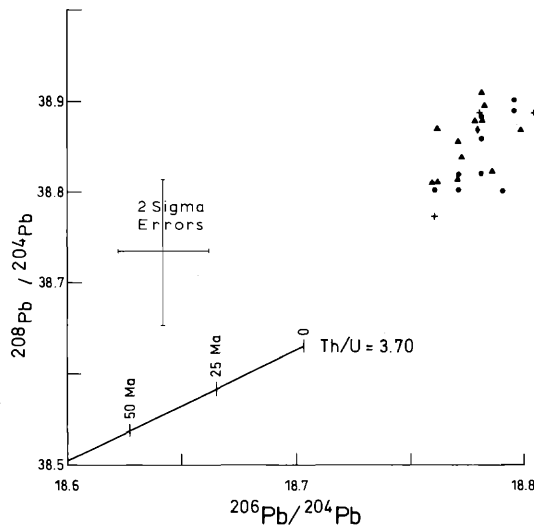


FIG. 21. Plot of $^{208}\text{Pb}/^{204}\text{Pb}$ vs. $^{206}\text{Pb}/^{204}\text{Pb}$ ratios of average galenas from Olympias (●), Madem Lakos (▲), Mavres Petres (+), and concentrate (◆). Lead growth curve for average crust and isochron lines are from Stacey and Kramers (1975).

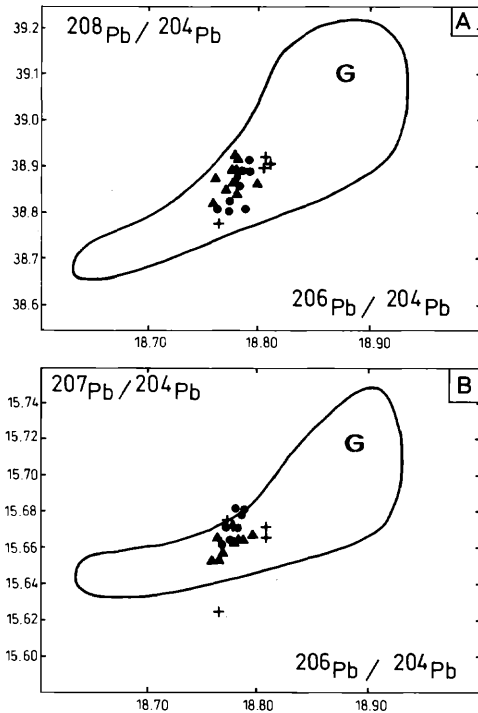


FIG. 22. Plots of $^{208}\text{Pb}/^{204}\text{Pb}$ (A) and $^{207}\text{Pb}/^{204}\text{Pb}$ (B) vs. $^{206}\text{Pb}/^{204}\text{Pb}$ ratios of average galenas from Olympias (●), Madem Lakos (▲), Mavres Petres (+), and concentrate (◆). The corresponding lead isotope composition of Greek K-feldspar (G) is from Juteau et al. (1986).

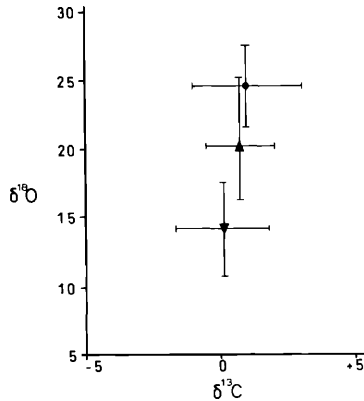


FIG. 23. Plot of $\delta^{18}\text{O}$ vs. $\delta^{13}\text{C}$ mean values for the upper nonore related (●), the lower ore host (▲) marble horizons, and ore-related calcites (▼). Solid lines represent one sigma (1σ) standard deviation.

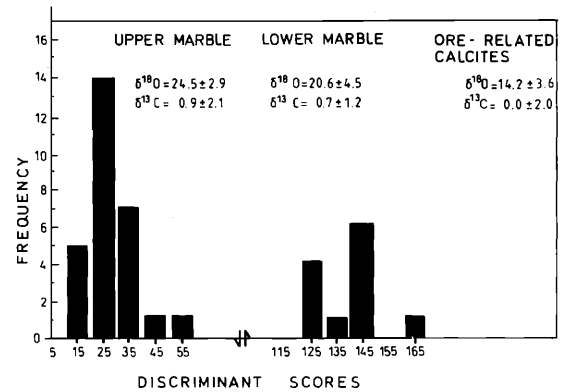


FIG. 24. Frequency diagram of discriminant scores obtained from a geochemical study of the upper relative to the lower marble horizons (Kalogeropoulos et al., 1989a), in relation to corresponding $\delta^{18}\text{O}$ and $\delta^{13}\text{C}$ data. Also the $\delta^{18}\text{O}$ and $\delta^{13}\text{C}$ values of ore-related calcites are shown (isotopic data expressed by mean ± 1 sigma, Table 7).

amphibolites point to a subalkaline basaltic-basaltic andesitic composition of tholeiitic affinity with mid-ocean ridge basaltlike parental characteristics. These rocks have been subjected to deformation and regional metamorphism at pressures ranging between 4 and 9 kbars and temperatures of 540° to 670°C. These metamorphics have subsequently been uplifted from Late Cretaceous to Tertiary. During uplift they have been intruded, at pressures approximately 1 to 5 kbars and temperatures of 350° to 550°C, by undeformed and deformed varieties of tonalitic-granitic pegmatite-aplite dikes, the 30-Ma Stratonis granodiorite, and calc-alkaline lamprophyre dikes. This stage is accompanied with, and followed by, retrogressing circulating fluids which deposited deformed and undeformed varieties of sulfide ores at pressures and temperatures of 0.3 and 0.8 kbars and 300° to 400°C, respectively, as evidenced by fluid inclusions. All the above P-T data are summarized in Figure 25.

2. The Olympias sulfide ores are strata bound, or fault controlled, hosted by the lower marble horizon along the contact with the overlying biotite gneiss and within the marble. The undeformed ores consti-

tute the largest part of the deposit and have cavity-filling, banded, vein or veinletlike, and disseminated form. The deformed ore units include some parts of the banded ore and the veins and are characterized by brecciation, mylonitization, folding, and shearing.

3. Pyrite, sphalerite, galena, arsenopyrite, and chalcopyrite constitute the main ore minerals, whereas quartz, calcite, and rhodochrosite are the gangue minerals. This mineral assemblage is present in both the undeformed and deformed ore varieties. All sphalerites show similar chemistry and fine zoning, regardless of deformation, suggesting that they belong to the same metallogenic system, and were deposited after the onset of the amphibolite regional metamorphism.

4. The Cu-Pb-Zn, Cu-Pb+Zn-Ag $\times 10^3$ bulk ore chemistries and Pb-Ag relations regardless of deformation point to a similarity to the eastern Chalkidiki sulfide ore deposits with the skarn replacement type.

5. Fluid inclusion data indicate that both undeformed and deformed ore types at Olympias were formed from H₂O-rich CO₂-bearing fluids with low

TABLE 7. Oxygen and Carbon Isotope Composition of Calcites from the Upper and Lower Marble Horizons of the Kerdilia Formation and the Orebodies of the Olympias Deposit

	$\delta^{18}\text{O}_{\text{smow}}$ (‰)			$\delta^{13}\text{C}_{\text{PDB}}$ (‰)		
	\bar{X}	1σ	Range	\bar{X}	1σ	Range
Upper marble ($n^1 = 17$)	24.5	2.9	17.4 to 28.9	0.9	2.1	-3.5 to 4.1
Ore-host lower marble ($n = 19$)	20.6	4.5	14 to 27.6	0.7	1.2	-2.6 to 2.3
Hydrothermal calcites ($n = 12$)	14.2	3.6	7.8 to 20.3	0.0	2	-3.8 to 2.4

¹ Number of measurements

TABLE 8. Oxygen Isotope Data of Ore-Related Quartz and Calcite and Corresponding Equilibrium Fluid at 350°C

Mineral	$\delta^{18}\text{O}_{\text{SMOW}}$ (‰)			$\delta^{18}\text{O}_{\text{SMOW,fluid}}$ (‰)		
	Mean	1 σ	Range	Mean	1 σ	Range
Quartz	15.1	2.6	12.1 to 19.3	9.8	2.6	6.8 to 14.0 ¹
Calcite	14.2	3.6	7.8 to 20.3	8.6	4.1	3.5 to 16.0 ²

¹ Fractionation equation of Matsuhisa et al. (1979)

² Fractionation equation of Friedman and O'Neil (1977).

to medium salinities of mean values between 2.5 and 6.5 equiv wt percent NaCl at 300° to 400°C temperatures and 300 to 800 bars pressure. Preliminary fluid inclusion data at Madem Lakos show even higher temperatures (homogenization up to 480°C) and complex salt (NaCl-KCl-CaCl₂) contents. These combined with ore chemistries may suggest that the Olympias deposit could be considered as a distal and the Madem Lakos as a proximal phase in a skarn replacement hydrothermal system. (Einaudi et al., 1981)

6. The narrow range of sulfur isotope ratios in all the sulfides, and their proximity to 0 per mil combined with the relatively limited occurrence of sulfates (e.g., gypsum) at Madem Lakos, may suggest the combined effects of high reduced oxidized/sulfur species ratios, relatively high temperature, and low $\delta^{34}\text{S}_{\text{initial}} - \delta^{34}\text{S}_{\text{H}_2\text{S}}$ values, thus suggesting an igneous origin for the sulfur.

7. On the basis of (1) the largely homogeneous isotopic signature of the ore leads regardless of whether they occur in deformed or undeformed marbles, or in veins; (2) the crustal affinity of lead; and (3) the similarity of the ore leads with the K feldspar lead from the nearby Tertiary orogenic granites, we may conclude that even if an older mineralization was present within the crustal rocks the lead must have been remobilized and thoroughly mixed, presumably in Tertiary magmas, in order to provide an extensive reservoir for lead. However some leaching of lead from crustal rocks by circulating fluids cannot be completely ruled out.

8. Oxygen and carbon isotope depletions in ore-related calcites compared to the hydrothermally altered ore-host lower marble and the unaltered upper marble horizons, primarily indicate oxygen isotope exchange between H₂O-dominated infiltrating ore-forming fluids and the host marble during sulfide ore deposition. The oxygen isotope composition of these fluids is consistent with either a magmatic and/or metamorphic origin with late involvement of meteoric waters.

9. On the basis of all the above data, a primarily magmatic fluid source is favored for the formation of both deformed and undeformed sulfide ore types.

Acknowledgments

We wish to thank H. N. A. Priem and J. Prevosteau for the lead isotope analyses and P. Pasteels, P. M. Holm, and B. Buchardt for their help with the oxygen and carbon isotope analyses. Thanks are also due to R. W. Hutchinson and an anonymous *Economic Geology* reviewer for their constructive criticism. This paper is published with the permission of C. Papavasiliou, Director General of the Institute of Geology and Mineral Exploration.

REFERENCES

- Altherr, R., Keller, J., Harre, W., Moehndore, A., Kreuzer, H., Lenz, H., Raschka, H., and Wendt, J., 1976, Geochronological data on granitic rocks of the Aegean Sea. Preliminary results: Internat. Symposium on the History of the Mediterranean Basins, Yugoslavia, 1976, Proc., p. 317-318.
- Bachinski, S. W., and Scott, R. B., 1979, Rare-earth and other trace element contents and the origin of minettes (mica-lamprophyres): *Geochim. et Cosmochim. Acta*, v. 43, p. 93-100.
- Barton, P. B., Jr., 1978, Some ore textures involving sphalerite from the Furutobe mine, Akita Prefecture, Japan: *Mining Geology*, v. 28, p. 293-300.
- Barton, P. B., Jr., and Toulmin, P., 1966, Phase relations involving sphalerite in the Fe-Zn-S system: *ECON. GEOL.*, v. 61, p. 815-849.
- Chalkias, S., and Vavelidis, M., 1988, Interpretation of lead isotope data from Greek Pb-Zn deposits based on an empirical two-stage model [abs.]: *Geol. Soc. Greece, Cong.*, 4th, May 1988, Athens, Greece, Abstracts, p. 36.
- Clayton, R. N., and Mayeda, T. K., 1963, The use of bromine pentafluoride in the extraction of oxygen from oxides and sil-

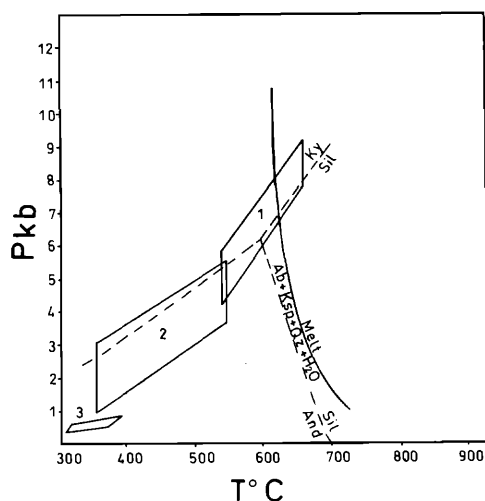


FIG. 25. The P-T conditions of metamorphism of biotite gneisses from Kerdilia (1), pegmatite emplacement (2), and ore deposition at Olympias (3). The stability areas of And-Ky-Sil, and the solidus of a H₂O-saturated granitic system, from Winkler (1979), are also shown.

- icates for isotopic analysis: *Geochim. et Cosmochim. Acta*, v. 27, p. 43–52.
- De la Roche, H., 1968, *Géochimie-comportement différentiel de Na, K et Al dans les formations volcaniques et sédimentaires: Un guide pour l'étude des formations métamorphiques et plutoniques*: Acad. Sci. [Paris], Comptes Rendus, v. 267, p. 39–42.
- Dimitriadis, S., 1974, Petrological studies of the migmatitic gneisses and amphibolites from the Redina-Asprovalta areas: Unpub. Ph.D. thesis, Thessaloniki, Greece, Univ. Thessaloniki, 168 p., (in Greek with English abs.).
- Dixon, J. E., and Dimitriadis, S., 1985, Metamorphosed ophiolitic rocks from the Servo-Macedonian Massif, near Lake Volvi, north-east Greece, in Dixon, J. E., and Robertson, A. H. F., eds. *The geological evolution of the eastern Mediterranean*, Special Publication of the Geological Society, n. 17: Oxford, Blackwell Sci. Pub., p. 603–618.
- Doe, B. R., and Zartman, R. E., 1979, Plumbotectonics, the Phanerozoic, in Barnes, H. L., ed., *Geochemistry of hydrothermal ore deposits*: New York, Wiley Intersci., p. 22–70.
- Einaudi, M. T., Meinert, L. D., and Newberry, R. J., 1981, Skarn deposits: *ECON. GEOL. 75TH ANNIV. VOL.*, p. 317–391.
- Fournarakis, A., 1981, Contribution to the mineralogical and petrological study of amphibolitic rocks of the Servo-Macedonian Massif: Unpub. Ph.D. thesis, Thessaloniki, Greece, Univ. Thessaloniki, 231 p., (in Greek with English abs.).
- Franklin, J. M., Lydon, J. W., and Sangster, D. F., 1981, Volcanic-associated massive sulfide deposits: *ECON. GEOL. 75TH ANNIV. VOL.*, p. 485–627.
- Friedman, I., and O'Neil, J. R., 1977, Compilation of stable isotope fractionation factors of geochemical interest: U. S. Geol. Survey Prof. Paper 440-KK, 12 p.
- Garrels, R. M., and Mackenzie, F. T., 1971, *Evolution of sedimentary rocks*: New York, W. W. Norton Co., 397 p.
- Gustafson, L. B., and Williams, N., 1981, Sediment-hosted stratiform deposits of copper, lead, zinc: *ECON. GEOL. 75TH ANNIV. VOL.*, p. 139–178.
- Hodgson, C. J., and Lydon, J. W., 1977, The geological setting of volcanogenic massive sulfide deposits and active hydrothermal systems: Some implications for exploration: *Canadian Mining Metallurgy Bull.*, v. 70, p. 95–106.
- Ishihara, S., 1974, Geology of Kuroko deposits: *Soc. Mining Geologists Japan Spec. Issue 6*, p. 1–435.
- Juteau, M., Michard, A., and Albarede, F., 1986, The Pb-Sr-Nd isotope geochemistry of some recent circum-Mediterranean granites: *Contr. Mineralogy Petrology*, v. 92, p. 331–340.
- Kajiwara, Y., and Krouse, K. R., 1971, Sulfur isotope partitioning in metallic sulfide systems: *Canadian Jour. Earth Sci.*, v. 8, p. 1397–1408.
- Kalogeropoulos, S. I., and Arvanitidis, N. D., 1988, A comparison of the chemistry of sphalerites between the Pb-Zn(Au,Ag) sulfide deposits of the Eastern Chalkidiki Peninsula and the respective mineralizations of the Thermes area, Xanthi, N. Greece [abs.]: *Geol. Soc. Greece Cong.*, 4th, Athens, May 1988, Abstracts, p. 55.
- Kalogeropoulos, S. I., and Economou, G., 1987, A study of carbonate sphalerites from the carbonate-hosted Pb-Zn sulfide deposits of the eastern Chalkidiki Peninsula, Northern Greece: *Canadian Mineralogist*, v. 25, p. 639–646.
- Kalogeropoulos, S. I., and Kiliass, S. P., 1988, Oxygen (^{18}O) and carbon (^{13}C) isotopic changes of carbonate rocks and minerals in relation to the sulfide Pb,Zn(Au,Ag) mineralization of Olympias, E. Chalkidiki, N. Greece. Contribution to metallogeny and exploration [abs.]: *Geol. Soc. Greece Cong.*, 4th, May 1988, Athens, Greece, Abstracts, p. 54.
- Kalogeropoulos, S. I., and Theodoroudis, A., 1988, K/Ar and Rb/Sr of the minerals biotite, muscovite and amphibole from rocks of the Servo-Macedonian Massif, N. Greece: Unpub. report, I.G.M.E., Athens, Greece, 14 p. (in Greek with English abs.).
- Kalogeropoulos, S. I., Bitzios, D., Eliopoulos, D., and Veranis, N., 1987, Geological, mineralogical and geochemical study of the Olympias type Pb-Zn(Au,Ag) sulfide ore deposit, E. Chalkidiki, N. Greece. Contribution to its Metallogeny: *Mineral Deposits Research*, No. 19, I.G.M.E., Athens, 36 p. (in Greek with English abs.).
- Kalogeropoulos, S. I., Economou, G. S., Gerouki, F., Karamanou, E., Kougoulis, C., and Perlikos, P., 1988a, Mineralogy and geochemistry of the Stratonian granodiorite and its metallogenetic significance: Unpub. report, I.G.M.E., Athens, Greece, 20 p. (in Greek with English abs.).
- Kalogeropoulos, S. I., Gerouki, F., and Papadopoulos, C., 1988b, Mineralogy, geochemistry, genesis and metallogenetic significance of lamprophyres from the Stratonian-Olympias area, Kerdilia Formation, E. Chalkidiki: Unpub. report, I.G.M.E., Athens, Greece, 22 p. (in Greek with English abs.).
- Kalogeropoulos, S. I., Chorianopoulos, E., Bitzios, D., and Hellingwerf, R., 1989a, A study of the mineralogical and geochemical changes of the Kerdilia marbles in relation to the Pb-Zn(Au,Ag) sulfide ore deposits: Unpub. report, I.G.M.E., Athens, Greece, 21 p. (in Greek with English abs.).
- Kalogeropoulos, S. I., Gerouki, F., Papadopoulos, C., and Foliadis, D., 1989b, Geological mineralogical and geochemical study of pegmatites from the Kerdilia Formation, E. Chalkidiki—Origin and metallogenetic significance: Unpub. report, I.G.M.E., Athens, Greece, 20 p. (in Greek with English abs.).
- Kiliass, S. P., and Kalogeropoulos, S. I., 1988, Physicochemical conditions during ore formation of the Olympias Pb-Zn(Au,Ag) massive sulfide ore deposit, Chalkidiki Peninsula, N. Greece [abs.]: *Geol. Soc. Greece Cong.* 4th, May 1988, Athens, Greece, Abstracts, p. 64.
- Kockel, F., Mollat, H., and Walther, H. W., 1977, Erläuterungen zur geologischen Karte der Chalkidiki und angrenzender gebiete 1:100.000 (Nord-Griechenland): Bundesamt. Geowiss. Rohst., Hannover, 119 p.
- Liati, A., 1986, Regional metamorphism and overprinting contact metamorphism of the Rhodope Zone near Xanthi (N. Greece): *Petrology, geochemistry, geochronology*: Unpub. Ph.D. thesis, Techn. Univ. Braunschweig, 186 p.
- Lydon, J. W., 1977, The significance of metal ratios in hydrothermal ore deposits: Unpub. Ph.D. thesis, Kingston, Ontario, Queen's Univ., 601 p.
- 1983, Chemical parameters controlling the origin and deposition of sediment-hosted stratiform lead-zinc deposits: *Mineralog. Assoc. Canada, short course, Handbook*, v. 9, p. 175–245.
- Matsuhisa, Y., Goldsmith, J. R., and Clayton, R. N., 1979, Oxygen isotopic fractionation in the system quartz-albite-anorthite-water: *Geochim. et Cosmochim. Acta*, v. 43, p. 1131–1140.
- McCrea, J. M., 1950, The isotope chemistry of carbonate and a paleotemperature scale: *Jour. Chem. Physics*, v. 18, p. 849–857.
- McNeil, A. M., and Kerrich, R., 1985, Archean lamprophyre dykes and gold mineralization, Mathieson, Ontario: The conjunction of LILE-enriched mafic magmas, deep crustal structures and Au mineralization: *Canadian Jour. Earth Sci.*, v. 23, p. 324–343.
- Neubauer, W. H., 1956, Der zyklische magmatismus auf der Chalkidiki und seine erzlagerstätten: *Berg Hüttenm. Monatsh.*, 102, p. 164–169.
- 1957, Geologie der blei-zink reichen kieslagerstätten von Kassandra (Chalkidiki-Griechenland): *Berg Hüttenm. Monatsh.*, v. 102, p. 1–16.
- Nicolaou, M., 1960, L'intrusion granitique dans la région de Stratonian-Olympiade et sa relation avec la métallogénèse: *Annales Géol. Pays Helléniques*, v. 11, p. 214–265.

- 1964, Mineralogy and micrography of the sulfide ores of the Kassandra mines, Greece: *Annales Géol. Pays Helléniques*, v. 16, p. 111–139.
- 1971, On the composition of the Kassandra mines ore bodies: *Praktika Akad. Athens*, v. 44, p. 82–93 (in Greek).
- Nicolaou, M., and Kokonis, I., 1980, Geology and development of the Olympias mine, eastern Chalkidiki, Macedonia, Greece, in Jones, M. J., ed., *Complex sulfides ores*: London, Inst. Mining Metallurgy, p. 260–270.
- Ohmoto, H., 1972, Systematics of sulfur and carbon isotopes in hydrothermal ore deposits: *ECON. GEOL.*, v. 67, p. 551–578.
- Ohmoto, H., and Rye, R. O., 1979, Isotopes of sulfur and carbon, in Barnes, H. L., ed., *Geochemistry of hydrothermal ore deposits*: New York, Wiley Intersci., p. 509–567.
- Papadakis, A., 1971, On the age of granitic intrusion, Chalkidiki (Greece): *Annales Géol. Pays Helleniques*, v. 23, p. 297–300 (in Greek).
- Papadopoulos, C., 1982, *Geologie des Servo-Mazedonischen Massivs, nordlich des Volvi-See, N. Griechenland*: Unpub. Ph.D. thesis, Univ. Wien, 176 p.
- Papadopoulos, C., and Kiliass, A., 1985, Altersbeziehungen zwischen metamorphose und deformation im zentralen teil des Serbomazedonischen Massivs (Vertiskos Gebirge, Nord-Griechenland): *Geol. Rundschau*, v. 74, p. 77–85.
- Patras, D., Kiliass, A., Chadzidimitriadis, E., and Mundrakis, D., 1986, Study of the deformation phases of the internal Hellenides in Northern Greece: *Geol. Soc. Greece Bull.*, v. 20, p. 139–157 (in Greek with English abs.).
- Rock, N. M. S., 1984, Nature and origin of calcalkaline lamprophyres: Minettes, vogesites, kersantites and spessartites: *Royal Soc. Edinburgh Earth Sci. Trans.*, v. 74, p. 193–277.
- Rock, N. M. S., Duller, R. S., Haszeldine, R. S., and Groves, D. I., 1987, Lamprophyres as potential gold exploration targets: Some preliminary observations and speculations: *Univ. Western Australia, Geology Dept. Univ. Ext.*, Pub. 11, p. 271–286.
- Rye, R. O., and Ohmoto, H., 1974, Sulfur and carbon isotopes and ore genesis: A review: *ECON. GEOL.*, v. 69, p. 826–842.
- Sakai, H., 1968, Isotopic properties of sulfur compounds in hydrothermal processes: *Geochem. Jour. (Japan)*, v. 2, p. 29–49.
- Sakellariou, D. T., 1988, Deformation and metamorphism of the Servo-Macedonian massif in north-east Chalkidiki, northern Greece [abs.]: *Geol. Soc. Greece, Congress, 4th, Athens, May 1988, Abstracts*, p. 44.
- Salmon, B. C., Clark, B. R., and Kelly, W. C., 1974, Sulfide deformation studies II: Experimental deformation of galena to 2,000 bars and 400°C: *ECON. GEOL.*, v. 69, p. 1–16.
- Sangster, D. F., and Scott, S. D., 1976, Precambrian stratabound massive Cu-Zn-Pb sulfide ores of North America, in Wolf K. H., ed., *Handbook of stratabound and stratiform ore deposits*: Amsterdam, Elsevier, p. 129–222.
- Sengor, A. M. C., Yilmaz, Y., and Sungurlu, O., 1985, Tectonics of the Mediterranean Cimmerides: Nature and evolution of the western termination of the Paleotethys, in Dixon, J. E., and Robertson, A. H. F., eds., *The geological evolution of the eastern Mediterranean*: Oxford, Blackwell Scientific Publications, p. 603–618.
- Scott, S. D., 1976, Application of the sphalerite geobarometer to regionally metamorphosed terranes: *Amer. Mineralogist*, v. 61, p. 661–670.
- Scott, S. D., and Barnes, H. L., 1971, Sphalerite geothermometry and geobarometry: *ECON. GEOL.*, v. 66, p. 653–669.
- Shaw, D. M., 1972, The origin of the Apsley gneiss: *Canadian Jour. Earth Sci.*, v. 9, p. 18–35.
- Shelton, K. L., and Rye, D. M., 1982, Sulfur isotopic compositions of ores from Mines Gaspé, Quebec: An example of sulphate-sulfide isotopic disequilibria in ore-forming fluids with applications to other porphyry-type deposits: *ECON. GEOL.*, v. 77, p. 1688–1709.
- Smith, J. W., Doolan, S., and McFarlane, E. F., 1977, A sulfur isotope geothermometer for the trisulfide system galena-sphalerite-pyrite: *Chem. Geology*, v. 19, p. 83–98.
- Smith, J. W., Burns, M. S., and Croxford, N. J. W., 1978, Stable isotope studies of the origins of mineralization at Mount Isa: *Mineral. Deposita*, v. 13, p. 369–381.
- Stacey, J. S., and Kramers, J. D., 1975, Approximation of terrestrial lead isotope evolution by a two-stage model: *Earth Planetary Sci. Letters*, v. 26, p. 207–221.
- Tsombos, P., 1988, Fracture pattern of the Chalkidiki peninsula, in LANDSAT (TM) images: Athens, Greece, IGME, Unpub. rept., 11 p. (in Greek with English abs.).
- Tsombos, P., and Karmis, P., 1988, Deep fracture pattern of the area between Axios and Strimon rivers (N. Greece) as detected on LANDSAT (TM) images: Athens, Greece, IGME, Unpub. rept., 21 p. (in Greek with English abs.).
- Van de Kamp, D. C., Leake, B. E., and Senior, A., 1976, The petrography and geochemistry of some Californian arkoses with application to identifying gneisses of metasedimentary origin: *Jour. Geology*, v. 84, p. 195–212.
- Winkler, H. G. F., 1979, *Petrogenesis of metamorphic rocks*: New York, Springer-Verlag, 348 p.